Title
EBI3 regulates the NK cell response to mouse cytomegalovirus infection

Journal
Proceedings of the National Academy of Sciences of the United States of America, 114(7)

ISSN
0027-8424

Authors
Jensen, Helle
Chen, Shih-Yu
Folkersen, Lasse
et al.

Publication Date
2017-02-14

DOI
10.1073/pnas.1700231114

Peer reviewed

EBI3 regulates the NK cell response to mouse cytomegalovirus infection

Helle Jensen[a], Shih-Yu Chen[b], Lasse Folkersen[c], Garry P. Nolan[b], and Lewis L. Lanier[a,d,1]

[a]Department of Microbiology and Immunology, University of California, San Francisco, CA 94143; [b]Department of Microbiology and Immunology, Stanford University, Palo Alto, CA 94304; [c]Department of Systems Biology, Center for Biological Sequence Analysis, Technical University of Denmark, Lyngby DK-2800, Denmark; and [d]Parker Institute for Cancer Immunotherapy, San Francisco, CA 94143

Contributed by Lewis L. Lanier, January 7, 2017 (sent for review November 1, 2016; reviewed by Michael A. Caligiuri and Daniel J. Cua)

Natural killer (NK) cells are key mediators in the control of cytomegalovirus infection. Here, we show that Epstein–Barr virus-induced 3 (EBI3) is expressed by human NK cells after NKG2D or IL-12 plus IL-18 stimulation and by mouse NK cells during mouse cytomegalovirus (MCMV) infection. The induction of EBI3 protein expression in mouse NK cells is a late activation event. Thus, early activation events of NK cells, such as IFNγ production and CD69 expression, were not affected in EBI3-deficient (*Ebi3*$^{-/-}$) C57BL/6 (B6) mice during MCMV infection. Furthermore, comparable levels of early viral replication in spleen and liver were observed in MCMV-infected *Ebi3*$^{-/-}$ and wild-type (WT) B6 mice. Interestingly, the viral load in salivary glands and oral lavage was strongly decreased in the MCMV-infected *Ebi3*$^{-/-}$ B6 mice, suggesting that EBI3 plays a role in the establishment of MCMV latency. We detected a decrease in the sustained IL-10 production by NK cells and lower serum levels of IL-10 in the MCMV-infected *Ebi3*$^{-/-}$ B6 mice. Furthermore, we observed an increase in dendritic cell maturation markers and an increase in activated CD8^{+} T cells. Thus, EBI3 dampens the immune response against MCMV infection, resulting in prolonged viral persistence.

natural killer cell | EBI3 | cytomegalovirus

Natural killer (NK) cells play an essential role in host defense against viral infections, particularly herpesviruses, such as cytomegalovirus (CMV) (1). During infection, NK cell activation is tightly controlled by the integration of signals derived from activating and inhibitory receptors, through the interaction with target or accessory cells, and from cytokine receptors. Several activating NK receptors exist, including the activating killer cell Ig-like receptors (KIRs) in humans, the activating Ly49 receptors in rodents, NKG2D, the natural cytotoxicity receptors (i.e., NKp30, NKp44, and NKp46), and the activating Fc receptor CD16 (2). The activating receptors recognize either stress-induced ligands on viral-infected cells, virus-encoded proteins, or Ig-coated cells. Signals from the activating receptors promote cytoskeletal rearrangements and proliferation, as well as secretion of cytolytic granules and cytokines (2). The inhibitory receptors Ly49 and KIR recognize polymorphic major histocompatibility complex class I ligands that can dampen or prevent the NK cells from attacking self (2).

NK cell-mediated control of viral infections has been studied extensively in mice infected with mouse CMV (MCMV). NK cells contribute directly to the early control of MCMV infection by eliminating the virus-infected cells. In C57BL/6 (B6) mice, Ly49H^{+} NK cells recognize MCMV-infected cells expressing the virus-encoded protein m157. This antigen-specific recognition leads to NK cell activation (3), as well as expansion and differentiation of memory NK cells (4), which is dependent on the DAP12 adapter protein, the costimulatory receptor DNAM-1, and the proinflammatory cytokine IL-12 (4–6). The DAP10 adapter protein and the cytokines IL-33 and IL-18 are required for optimal expansion of Ly49H^{+} NK cells, but not for memory NK cell differentiation (7–9). In addition, optimal activation of both Ly49H^{+} and Ly49H^{-} NK cells and production of IFNγ during MCMV infection is critically dependent on both IL-12 and IL-18 (9, 10). In addition to mediating early control of MCMV infection, NK cells also play a role in shaping the subsequent adaptive immune responses. Crosstalk between NK cells and dendritic cells (DCs) early during MCMV infection affects the outcome of the T-cell responses. IL-10 secreted by various immune cells, including NK cells, dampens the T-cell response by negatively affecting the maturation of DCs, and in the absence of IL-10 secretion of IFNγ and TNFα by NK cells enhances the maturation of DCs, which boosts the T-cell response (11).

The cytokine Epstein–Barr virus-induced 3 (EBI3) was first identified in B cells infected with Epstein–Barr virus (12), but several other cells from the immune system have also been found to express and secrete EBI3, including activated DCs, regulatory T cells, and regulatory B cells (13–15). EBI3 belongs to the IL-12 family of cytokines that consists of the four heterodimeric cytokines IL-12 (p35/p40), IL-23 (p19/p40), IL-27 (p28/EBI3), and IL-35 (p35/EBI3), which signal through unique pairings of the five receptor chains IL-12Rβ1, IL-12Rβ2, IL-23R, gp130, and WSX-1 (16). IL-27 and IL-35 lack disulfide linkage and pair poorly and are therefore less stable and secreted in much lower amounts than the disulfide-linked family members IL-12 and IL-23 (16). It has been well-documented that IL-12 and IL-23 function as proinflammatory cytokines. However, studies with IL-27 and IL-35 have been complicated by their instability in solution and the lack of specific reagents. IL-27 has been proposed to possess both proinflammatory and anti-inflammatory properties in that it can promote Th1 polarization (17) but also stimulate the production of IL-10 (18, 19). IL-35 appears to possess anti-inflammatory properties with the predominant mechanism being suppression of T-cell proliferation and conversion of naive T cells into IL-10–producing

Significance

Natural killer (NK) cells play a key role in early viral control of CMV replication and in shaping the adaptive immune response. Despite an early control, CMV persists by exploiting host immune inhibitory pathways. Here, we describe a previously unidentified pathway wherein the cytokine Epstein–Barr virus-induced 3 (EBI3) affects the establishment of mouse cytomegalovirus (MCMV) latency. We also show that both human and mouse NK cells express EBI3 and the EBI3 receptor, gp130, after stimulation. MCMV-infected EBI3-deficient mice showed decreased IL-10 production by NK cells, increased dendritic cell maturation and activation of CD8^{+} T cells, and significantly diminished viral loads in the salivary glands and oral lavage. Together, our results provide insight into how CMV establishes latent infection.

Author contributions: H.J. and L.L.L. designed research; H.J. and S.-Y.C. performed research; S.-Y.C., L.F., and G.P.N. contributed new reagents/analytic tools; H.J., S.-Y.C., L.F., and L.L.L. analyzed data; and H.J. and L.L.L. wrote the paper.

Reviewers: M.A.C., Ohio State University; and D.J.C., Merck Research Laboratory, Palo Alto, CA.

Conflict of interest statement: L.L.L. and the University of California, San Francisco have licensed intellectual property rights regarding NKG2D for commercial applications.

[1]To whom correspondence should be addressed. Email: lewis.lanier@ucsf.edu.

This article contains supporting information online at www.pnas.org/lookup/suppl/doi:10.1073/pnas.1700231114/-/DCSupplemental.

T cells (13). It has been speculated that EBI3 can be secreted and function as a homodimer; however, this remains to be elucidated (15, 16). Here we identify activated human and mouse NK cells as producers of EBI3 and show that EBI3 promotes the persistence of MCMV infection.

Results

Gene Expression Analysis of NKL Cells Stimulated Through Activating Receptors. We investigated the global gene expression profile of human NK cells stimulated through various activating receptors to identify genes involved in the regulation of NK cell functions. We used the human-transformed NK cell line, NKL, stably transduced with either the activating mouse Ly49H receptor or the activating human KIR2DS1 receptor (Fig. S1*A*). NKL cells, which constitutively express the activating NKG2D receptor (Fig. S1*A*), were stimulated with saturating amounts of plate-bound isotype-matched control Ig or receptor-specific monoclonal antibodies (mAbs), and the RNA was extracted and used for deep sequencing. Before analysis the quality of the gene expression data was verified using principal component analysis (PCA) and by calculating the Pearson correlation coefficient for the experimental replicates (Fig. S1 *B* and *C*).

In our gene expression analysis of the activated NKL cells, we scrutinized genes that were up- and down-regulated with at least a 1.5-fold change relative to the control samples. A total of 254, 158, or 596 genes were identified to be up- and down-regulated 4 h after KIR2DS1, NKG2D, or Ly49H stimulation, respectively (Fig. 1*A* and Dataset S1). We examined the 133 genes that were commonly regulated by all three stimulations (Fig. 1*A*) by gene set enrichment analysis (GSEA). GSEA is a pathway-based analysis that detects changes in expression of genes in entire pathways or gene sets and is therefore more robust than analyses based upon individual genes. GSEA identified 20 gene sets and pathways that were significantly different relative to the control samples (Fig. 1*B*). The gene set with the highest enrichment score identified by GSEA was "cytokines," which included many genes known to be expressed by activated NK cells, i.e., *IFNG*, *FASLG*, *XCL1*, *CCL1*, *CCL3*, *CCL4*, and *CCL5* (2, 20, 21) (Fig. 1*C*). Interestingly, we detected an up-regulation of *EBI3* in the activated NKL cells (Fig. 1*C*). *EBI3* expression has recently been shown to be up-regulated in human NK cells in response to Fc receptor activation, but only in the presence of IL-12 (22), confirming our results that activated NK cells can express *EBI3*; however, to our knowledge no previous studies have examined EBI3 protein expression and secretion by human and mouse NK cells. Furthermore, the effect of EBI3 on NK cell function in vivo is unknown.

EBI3 Protein Expression and Secretion Is Increased in Human NK Cells in Response to Receptor- and Cytokine-Mediated Stimulation. NKL cells constitutively express *EBI3*, which was significantly increased upon receptor-mediated stimulation (Fig. 2*A*). *IL12A* (i.e., p35) was also constitutively expressed in NKL cells, but its expression was not increased after receptor-mediated stimulation (Fig. 2*A*). In agreement with the gene expression data, the majority of or all NKL cells express EBI3 and p35, respectively (Fig. 2*B*), and the amount of intracellular EBI3, but not p35, proteins was increased following receptor-mediated stimulation for 24 h (Fig. 2 *C* and *F*, respectively). In addition, the intracellular EBI3 protein level was increased in response to IL-12 plus IL-18 treatment for 24 h (Fig. 2*D*). EBI3 and p35 protein was found in the supernatant of NKL cells after culture, but only EBI3 secretion was increased after stimulation (Fig. 2 *E* and *G*), which was consistent with the intracellular protein levels observed. To confirm that EBI3 is also expressed by primary human NK cells, we examined the intracellular EBI3 protein level in resting and activated $CD56^{dim}$ (i.e., mature) and $CD56^{bright}$ (i.e., immature) NK cells derived from healthy human blood donors. Resting NK cells did not express EBI3 (Fig. S2 *A* and *B*), suggesting that the constitutive expression of EBI3 observed in NKL cells is due to cell transformation and/or the in vitro culture conditions. Treatment with IL-12 alone for 24 h did not induce EBI3 protein expression, and only a slight increase was observed after treatment with IL-18 alone (Fig. S2*A*). However, treatment with IL-12 in combination with IL-18 for 24 h led to a robust induction of EBI3 protein expression in both $CD56^{bright}$ and $CD56^{dim}$ NK cells (Fig. S2 *A* and *B*). Priming with IL-2 for 24 h did not induce EBI3 protein expression; however, a significant increase was observed after stimulation of IL-2–primed NK cells

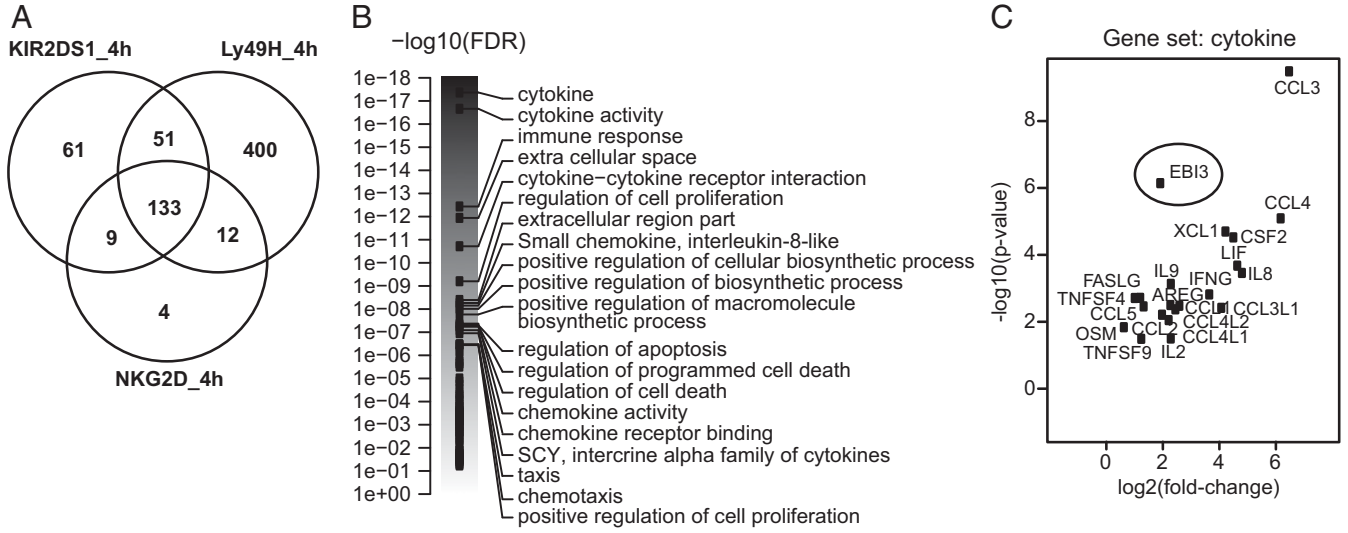

Fig. 1. Gene expression analysis of NKL cells stimulated through activating receptors. (*A*) RNA was isolated from NKL cells stimulated with the indicated plate-bound Abs for 4 h and then analyzed by deep sequencing. Shown is the number of genes that were up- and down-regulated with at least a 1.5-fold change in the receptor-stimulated NKL cells relative to the control-treated cells (n = 2–4 independent experiments). (*B* and *C*) GSEA was performed on the deep-sequencing data. (*B*) Shown are the strongest associated gene sets/pathways when analyzing genes that were significantly differentially expressed between NKG2D-stimulated NKL cells versus control-treated cells at 4 h. The scale is given as DAVID-reported –log10 (false discovery rate) value, i.e., the gene-set score. The score of all gene sets is shown, but only the top 20 are labeled. (*C*) Shown is a volcano plot of the genes contained in the "cytokine" gene set, which had the strongest enrichment score in *B*. The *x* axis indicates a log2 fold-change, with positive values corresponding to genes for which expression is up-regulated.

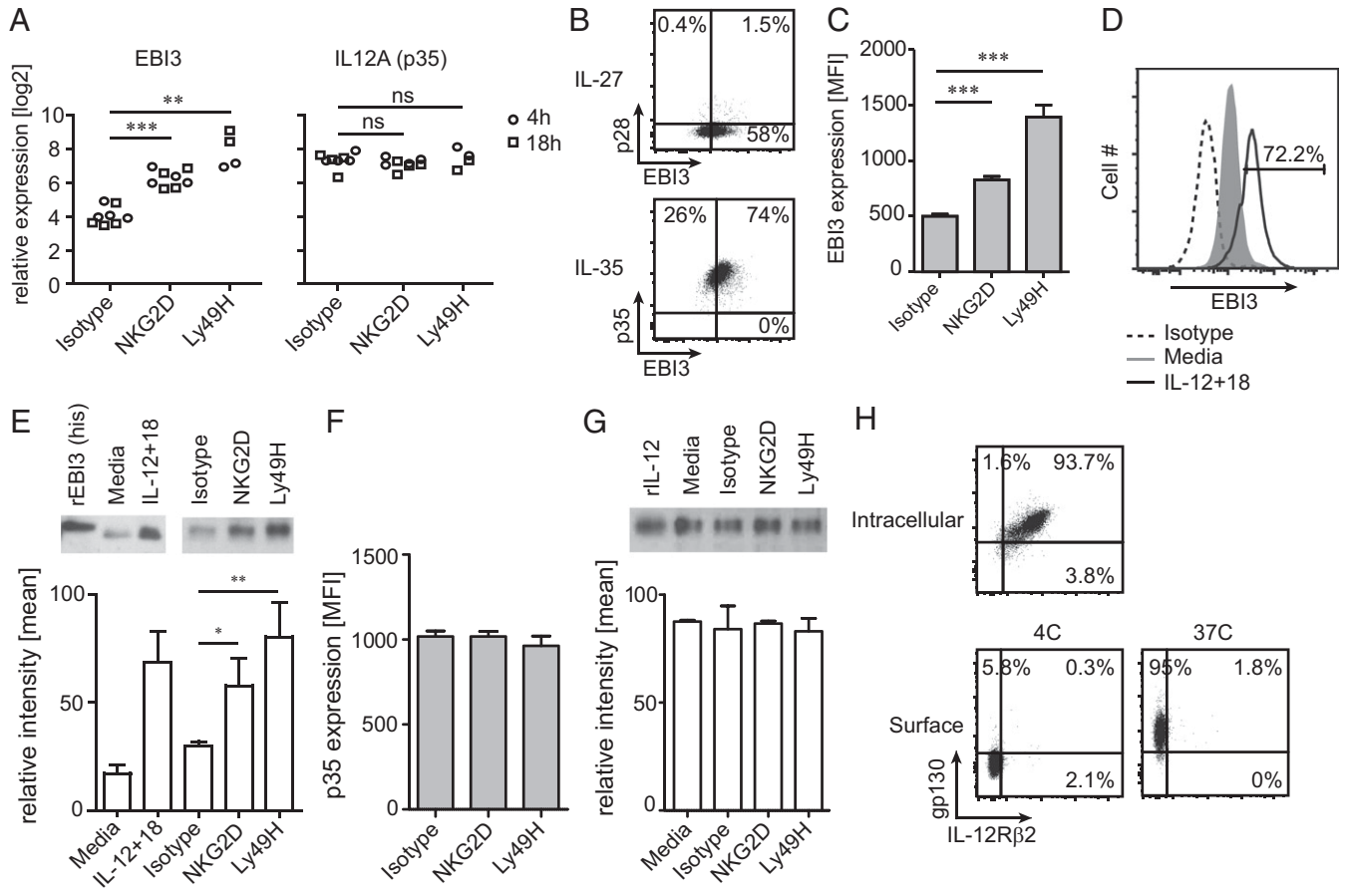

Fig. 2. EBI3 protein expression is increased in response to receptor- and cytokine-mediated stimulation. (*A*) Gene expression data for EBI3 and p35 in NKL cells stimulated with the indicated plate-bound Abs for 4 h (circle) or 18 h (square) were obtained from the deep-sequencing analysis (n = 2–4 independent experiments; statistical analysis is shown for 4-h samples). (*B*) Intracellular EBI3, p28, and p35 protein expression was examined by flow cytometry in resting NKL cells. Data are representative of three independent experiments. (*C* and *D*) Intracellular EBI3 protein expression was measured by flow cytometry in NKL cells stimulated with (*C*) plate-bound Abs or (*D*) IL-12+IL-18 for 24 h. (*C*) Data show mean ± SD from three independent experiments. (*D*) Data are representative of three independent experiments. (*E*) NKL cells were stimulated with plate-bound Abs, media, or IL-12+IL-18 for 24 h, and EBI3 was detected in the supernatant by Western blot analysis. The graphs show mean ± SD from two or three independent experiments. (*F*) Intracellular p35 protein expression was measured by flow cytometry in NKL cells stimulated with plate-bound Abs for 24 h. (*G*) NKL cells were stimulated with media or plate-bound Abs for 24 h, and p35 was detected in the supernatant by Western blot analysis. The graphs show mean ± SD from three independent experiments. (*H*) Surface and intracellular protein expression of gp130 and IL-12Rβ2 was examined by flow cytometry in resting NKL cells. Data are representative of three independent experiments. Statistical analysis was performed by two-tailed unpaired Student's t test (*P < 0.05, **P < 0.01, and ***P < 0.001).

with plate-bound anti-NKG2D mAb for 24 h (Fig. S2*C*). In contrast to EBI3 expression, the majority of resting NK cells constitutively expressed p35 (Fig. S2*A*). We did not detect any protein expression of p28 (Fig. 2*B*). NKL cells stained positive for both gp130 and IL-12Rβ2 as detected by intracellular protein staining (Fig. 2*H*, "intracellular"). Furthermore, gp130 was detected at the cell surface of NKL cells, but only after incubating the cells with the anti-gp130 Ab at 37 °C (Fig. 2*H*, "surface"), suggesting that the gp130 receptor is rapidly recirculated at the cell surface of the NKL cells. Resting primary human NK cells expressed low levels of gp130 at the cell surface, but the expression was increased in response to IL-12 plus IL-18 treatment, with the strongest induction observed in the $CD56^{bright}$ NK cells (Fig. S2*D*). Furthermore, the majority of $CD56^{bright}$ NK cells and all of the $CD56^{dim}$ NK cells constitutively expressed IL-12Rβ2 as detected by intracellular protein staining (Fig. S2*E*). No cell-surface staining of IL-12Rβ2 was detected by flow cytometry (Fig. 2*H*, "surface").

MCMV Infection Induces EBI3 Expression in Mouse NK Cells. Based on our results with human NK cells and the NKL cells transduced to express Ly49H, we examined if MCMV infection could be used as an in vivo model system to study the functional role of EBI3. During MCMV infection we detected an increase in the intracellular EBI3 protein level in splenic NK cells (Fig. 3 *A* and *B*), whereas no difference was detected in T cells, B cells, and DCs from the same samples (Fig. S3*A*). The increase in EBI3 protein expression in mouse NK cells was strongest at day 2.5 postinfection (p.i.) (Fig. 3*B*) with the highest levels observed in MCMV-specific $Ly49H^{+}$ (Fig. 3 *A* and *B*). The cell-surface expression of gp130 was increased on splenic NK cells in response to MCMV infection (Fig. 3 *C* and *D*), which indicates a possibility for an autocrine effect. This increase in gp130 surface expression was specific for NK cells, as the surface expression on T cells, B cells, and DCs was either decreased or unchanged (Fig. S3*B*). p35, but not p28, protein expression was increased in splenic NK cells in response to MCMV infection (Fig. 3 *E* and *F*), and like EBI3, the strongest induction of p35 protein expression was observed at day 2.5 p.i. (Fig. 3*E*).

EBI3-Deficient Mice Show Decreased MCMV Replication in the Salivary Glands and Oral Lavage. To examine the functional role of EBI3 in vivo, we infected wild-type (WT) and EBI3-deficient ($Ebi3^{-/-}$)

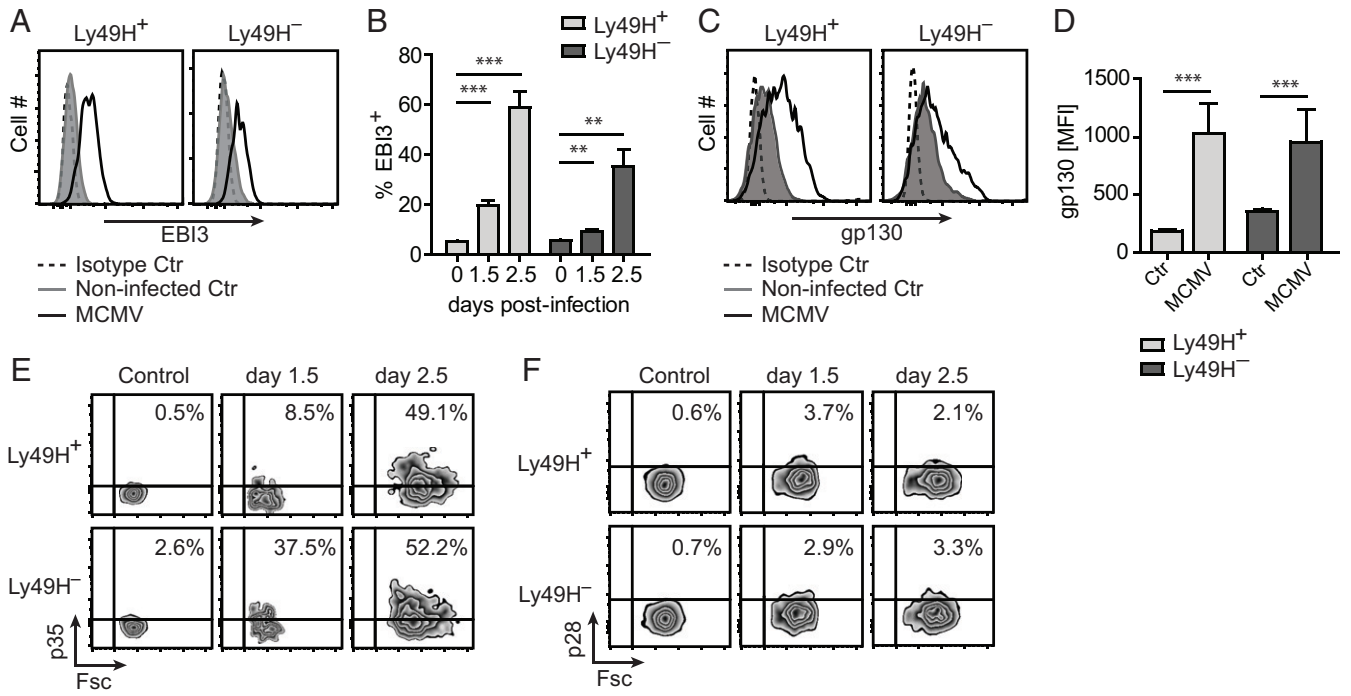

Fig. 3. MCMV infection induces EBI3 protein expression in mouse NK cells. Intracellular (*A* and *B*) EBI3, (*E*) p35, and (*F*) p28 protein expression was examined by flow cytometry in splenic Ly49H$^+$ and Ly49H$^-$ NK cells from noninfected and infected (day 1.5 and day 2.5) WT B6 mice. (*A*, *E*, and *F*) Data are representative of four mice for each time point from two independent experiments. (*B*) Data show mean ± SD from four or six mice for each time point from two independent experiments. (*C* and *D*) Surface expression of gp130 was examined by flow cytometry in splenic Ly49H$^+$ and Ly49H$^-$ NK cells from noninfected and MCMV-infected (day 2) WT B6 mice. (*C*) Data are representative of six mice from two independent experiments. (*D*) Data show mean ± SD from six mice from two independent experiments. Statistical analysis was performed by two-tailed unpaired Student's *t* test (**$P < 0.01$ and ***$P < 0.001$).

C57BL/6 (B6) mice with MCMV. The *Ebi3*$^{-/-}$ B6 mice lack exons 2–5 of the *Ebi3* gene, corresponding to amino acids 24–228 of the EBI3 protein (23), which includes the functional fibronectin type 3 domain found at amino acids 128–216 (24). Thus, the truncated version of EBI3 likely to be present in the deficient mice would be nonfunctional. No difference was observed between the two mouse strains with regard to the percentages of splenic NK cells and the immature and mature NK cell subsets (Fig. S4 *A* and *B*). Furthermore, the splenic NK cells showed similar expression levels of several NK receptors, including KLRG1, Ly49H, Ly49C/I, Ly49D, Ly49A, NKG2,A,C,E, NKp46, and NKG2D (Fig. 4*A* and Fig. S4*C*). Thus, EBI3 deficiency is not associated with any phenotypic or maturational defects in the NK cells. During MCMV infection, the early activation of splenic NK cells, measured by CD69 expression and IFNγ production at day 1.5 p.i., was comparable between the WT and *Ebi3*$^{-/-}$ B6 mice (Fig. 4 *B* and *C*, respectively). Furthermore, no difference in the viral load in liver and spleen from the mice was observed at day 4 p.i. (Fig. 4 *D* and *E*). We also observed a similar expansion of peripheral blood KLRG1^{hi} Ly49H$^+$ NK cells in the MCMV-infected mice (Fig. 4*A*). However, the viral load was significantly ($P < 0.05$) decreased in the blood in the MCMV-infected *Ebi3*$^{-/-}$ B6 mice at day 7 and day 14 p.i. (Fig. 4*F*). Interestingly, we found that MCMV was cleared most efficiently in the salivary glands and oral lavage of the *Ebi3*$^{-/-}$ B6 mice (Fig. 4 *G* and *H*), which are important sites for virus persistence and dissemination (25).

EBI3 Promotes IL-10 Production by NK Cells and Negatively Affects the Maturation of DCs and Activation of CD8$^+$ T Cells During MCMV Infection. Several cells in the immune system, including NK cells, produce IL-10 early after MCMV infection. The early production of IL-10 promotes virus replication in the salivary glands by negatively affecting the maturation of DCs, leading to poor priming of T cells (26, 27). We found that splenic Ly49H$^+$ and Ly49H$^-$ NK cells from the mice produced similar levels of IL-10 at day 2.5 post-MCMV infection (Fig. 5*A*). However, the IL-10 production was significantly decreased at day 3.5 p.i. in the *Ebi3*$^{-/-}$ B6 mice (Fig. 5*A*), suggesting that EBI3 plays an essential role in the sustained, but not initial, production of IL-10 by NK cells during MCMV infection. The serum level of IL-10 peaks at day 5 p.i. during MCMV infection (26). We found that the levels of IL-10 in sera were significantly decreased in the MCMV-infected *Ebi3*$^{-/-}$ B6 mice (Fig. 5*B*), indicating that the overall production of IL-10 was affected in the mice. We further examined the impact of EBI3 deficiency on DC maturation and T-cell activation, both of which are affected by IL-10 during MCMV infection (26, 27). We observed higher levels of the maturation markers CD86 and CD40 on splenic DCs derived from the *Ebi3*$^{-/-}$ B6 mice at day 5 p.i. (Fig. 5*C*). Furthermore, the percentage of activated peripheral CD8$^+$ T cells (i.e., NKG2D-positive CD8$^+$ T cells) was increased in the MCMV-infected *Ebi3*$^{-/-}$ B6 mice (Fig. 5*D*). Thus, together these results indicate that EBI3 promotes persistent MCMV infection, presumably in part by sustaining IL-10 production, which negatively affects the maturation of DCs and the activation of T cells.

Discussion

In this study, we show that both human and mouse NK cells express EBI3 protein after stimulation. Furthermore, we describe a previously unidentified pathway wherein EBI3 affects the establishment of MCMV latency. Interestingly, mice deficient in EBI3 showed almost no viral replication in salivary glands and oral lavage, which are the main sites for viral persistence and dissemination (25), whereas the early viral replication in the spleen and liver was comparable between the EBI3-deficient and WT mice. MCMV-infected mice displayed lower levels of IL-10 in the absence of EBI3, an effect that was observed in splenic NK cells at

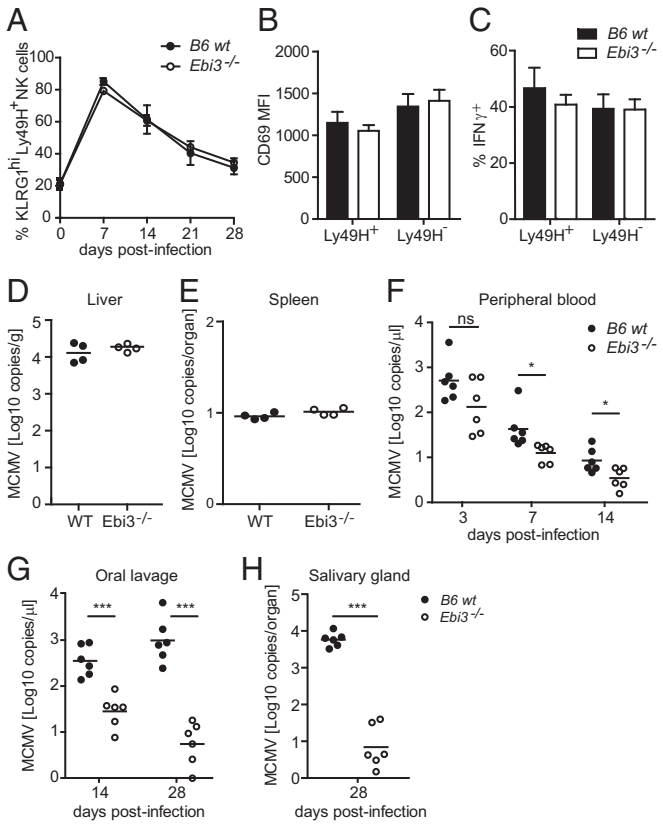

Fig. 4. EBI3-deficient mice show decreased MCMV replication in the salivary glands and oral lavage. (*A*) Expansion of peripheral KLRG1^{hi} Ly49H^{+} NK cells from WT or *Ebi3*$^{-/-}$ B6 mice was measured by flow cytometry at days 0, 7, 14, 21, and 28 p.i. $n = 6$ for each mouse strain and time point from two independent experiments (mean ± SD). (*B*) CD69 expression and (*C*) IFNγ production was measured by flow cytometry in splenic Ly49H^{+} and Ly49H^{-} NK cells from WT or *Ebi3*$^{-/-}$ B6 mice at day 1.5 post-MCMV infection. $n = 4$ for each mouse strain from two independent experiments. Data show mean ± SD. MCMV titer in WT or *Ebi3*$^{-/-}$ B6 mice was determined by real-time PCR in (*D*) liver and (*E*) spleen at day 4 p.i. in (*F*) peripheral blood at days 3, 7, and 14 p.i., in (*G*) saliva (by oral lavage) at day 14 and day 28 p.i., and (*H*) in salivary glands at day 28 p.i. $n = 4$ or 6 for each mouse strain and time point from two independent experiments. Statistical analysis was performed by two-tailed unpaired Student's *t* test (*$P < 0.05$ and ***$P \leq 0.0003$).

day 3.5 p.i. and in the serum at day 5 p.i. As reported previously, production of IL-10 early during MCMV infection is important for limiting DC maturation and T-cell activation to prevent harmful immune-mediated tissue damage in the host (26, 27). During MCMV infection, IL-10 production by NK cells and other immune cells can suppress the maturation DCs, leading to poor priming of CD4^{+} T cells (26). Furthermore, NK cell-mediated IL-10 production during MCMV infection regulates CD8^{+} T-cell activation, where a blockade of IL-10 increases the CD8^{+} T-cell response against MCMV (27). We detected an increase in both the maturation markers of DCs and the percentage of activated CD8^{+} T cells in the MCMV-infected EBI3-deficient mice, indicating that the observed decrease in IL-10 production in the EBI3-deficient mice was able to enhance the subsequent T-cell response. In this study we found that EBI3 affects the production of IL-10 by NK cells during MCMV infection, as measured by direct ex vivo intracellular staining for IL-10 protein. However, it remains to be determined whether the production of IL-10 by other cell subsets, such as myeloid cells and CD4^{+} T cells, is affected by EBI3 during MCMV infection. Although beyond the scope of this article, it is also possible that EBI3 plays an additional role(s) in MCMV latency that is independent of IL-10. Production of IL-10 early during MCMV infection depends on the magnitude of viral replication (28). Following a low-dose MCMV infection, viral replication is controlled rapidly within a couple of days and only low levels of IL-10 are produced to limit the immune response. In contrast, during a high-dose MCMV infection, which leads to sustained and elevated levels of viral replication, sustained and higher amounts of IL-10 are needed to limit the immune response and prevent tissue damage (28). Our data suggest that EBI3 is essential to sustain IL-10 production during a high-dose MCMV infection.

EBI3 can interact with p28 to form IL-27 heterodimers or with p35 to form IL-35 heterodimers (16). We detected p35, but never p28, protein expression in human and mouse NK cells. Both EBI3 and p35 were constitutively secreted by the NKL cells. Therefore, in our experimental settings activated NK cells do not produce or secrete IL-27 heterodimers. For several reasons we were not able to distinguish between IL-35 heterodimers and EBI3 homodimers and therefore were unable to determine which of the two species are predominantly formed and secreted by the activated NK cells. First, there are no blocking Abs that can distinguish between EBI3 and IL-35. Second, IL-35 is very unstable in solution (16), which makes the detection of small amounts by ELISA or immunoprecipitation difficult or impossible. Finally, mice deficient in p35 also lack IL-12, a cytokine essential for NK cell activation and proliferation in response to MCMV infection (6, 10). EBI3 protein and the gp130 receptor was up-regulated in splenic NK cells during MCMV infection, whereas no up-regulation was observed in T cells, DCs, or B cells at the time points examined in this study. However, the basal or background level differed between the

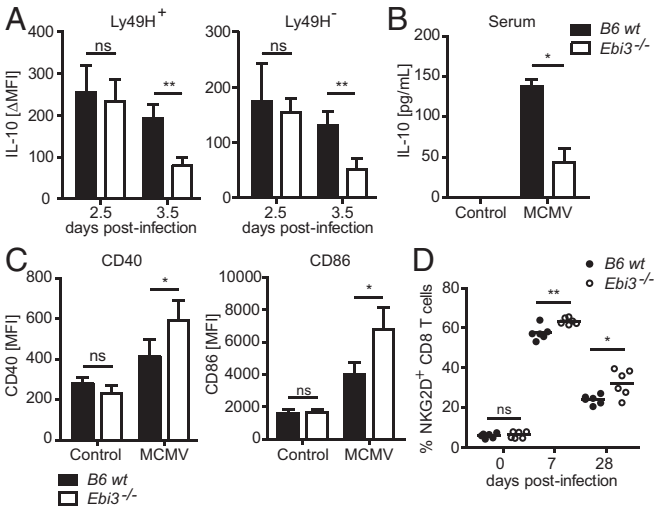

Fig. 5. EBI3 promotes IL-10 production by NK cells and negatively affects the maturation of DCs and activation of CD8^{+} T cells during MCMV infection. (*A*) IL-10 expression was measured by flow cytometry in splenic Ly49H^{+} and Ly49H^{-} NK cells from WT or *Ebi3*$^{-/-}$ B6 mice at day 2.5 and 3.5 p.i. $n = 4$ for each mouse strain from two independent experiments. Shown are the mean ± SD of the induced IL-10 mean fluorescence intensity (MFI) in MCMV-infected compared with noninfected control mice. (*B*) IL-10 was measured in sera from MCMV-infected (day 5) or noninfected WT or *Ebi3*$^{-/-}$ B6 mice by ELISA. Data are representative of four mice for each time point from two independent experiments. (*C*) CD40 and CD86 expression was measured by flow cytometry on splenic DCs from MCMV-infected (day 5) or noninfected control WT or *Ebi3*$^{-/-}$ B6 mice. $n = 4$ for each mouse strain from two independent experiments (mean ± SD). (*D*) NKG2D expression was measured on peripheral CD8^{+} T cells from WT or *Ebi3*$^{-/-}$ B6 mice by flow cytometry at days 0, 7, and 28 p.i. $n = 6$ for each mouse strain and time point from two independent experiments. Statistical analysis was performed by two-tailed unpaired Student's *t* test (*$P < 0.05$ and **$P < 0.01$).

various cell types examined. We cannot distinguish between the role of EBI3 derived from NK cells versus other cell types during MCMV infection as there presently is no conditional knockout of *Ebi3* to definitively address this issue.

The immune system has established multiple layers of control to ensure effective protection against viral infections, but at the same time to keep the immune system in check to avoid excessive inflammation and autoimmunity. NK cells play a key role in the early control of CMV replication and in modulating the adaptive immune response against the virus (1). Despite the cooperative work between NK cells and T and B cells, CMV can establish persistent infections in mice and humans by exploiting host immune inhibitory pathways to modulate the virus–host balance toward its own benefit (25). Induction of the regulatory cytokine IL-10 during infection represents one such immune inhibitory pathway (29). Our results suggest that the induction of EBI3 represents an inhibitory pathway that can be exploited by CMV to establish latent infection. Whether EBI3 can affect the persistent infection of other herpesviruses remains to be elucidated. However, it is noteworthy that Epstein–Barr virus, another virus that can establish latency by exploiting the IL-10 inhibitory pathway (25), is also a strong inducer of EBI3 expression (12).

Materials and Methods

WT and EBI3-deficient (B6.129 × $1^{Ebi3tm1Rsb/J}$) mice on a C57BL/6 background were maintained and used in accordance with guidelines of the University of California at San Francisco (UCSF) Institutional Animal Care and Use Committee. Peripheral blood mononuclear cells (PBMCs) were isolated from blood obtained from the Stanford Blood Center or the Blood Centers of the Pacific under an Institutional Review Board approved protocol (IRB# 10–00265) by density gradient centrifugation using Ficoll-Paque PLUS (GE Healthcare Bio-Sciences AB).

Reagents, vendors, and protocols are included in *SI Materials and Methods*. Details of the mice and cells used, as well as details of the methods used including MCMV infection, in vitro stimulation of NK cells, real-time PCR, flow cytometry, Western blot analysis, IL-10 ELISA, and deep sequencing are presented in *SI Materials and Methods*. Additional questions pertaining to methods, protocols, and reagents are available upon request.

ACKNOWLEDGMENTS. We thank the L.L.L. laboratory for comments and discussions; Viola Lam and Tsukasa Nabekura for assistance with MCMV infections; Melissa Lodoen for generating the Ly49H$^+$ NKL cells; Sandra Laurence Lopez-Verges for generating the KIR2DS1$^+$ NKL cells; Roberto Biassoni for providing the cDNA of human KIR2DS1; Hisashi Arase for providing the pMXs retroviral vector; Prometheus Laboratories, Inc., for providing human IL-2; and Novo Nordisk, Inc., for providing the deep-sequencing platform. L.L.L. is an American Cancer Society Professor and funded by National Institutes of Health Grants AI066897 and AI068129 and the Parker Institute for Cancer Immunotherapy. H.J. is supported by a Lundbeck Foundation Postdoctoral Fellowship. In addition, the work was supported by NIH Grants U19AI057229, U19AI100627, R33CA183654, R33CA0183692, R01GM10983601, R01CA184968, R01CA19665701, R21CA183660, R01NS08953301, 5UH2AR067676, and R01HL120724; the Northrop-Grumman Corporation; Novartis Grant CMEK162AUS06T; Pfizer Grant 123214; Juno Therapeutics Grant 122401; Department of Defense Grants OC110674 and W81XWH-14-1-0 180; Gates Foundation Grant OPP1113682; and Food and Drug Administration Grant BAA-15-00121.

1. Lanier LL (2008) Evolutionary struggles between NK cells and viruses. *Nat Rev Immunol* 8(4):259–268.
2. Lanier LL (2008) Up on the tightrope: Natural killer cell activation and inhibition. *Nat Immunol* 9(5):495–502.
3. Arase H, Mocarski ES, Campbell AE, Hill AB, Lanier LL (2002) Direct recognition of cytomegalovirus by activating and inhibitory NK cell receptors. *Science* 296(5571):1323–1326.
4. Sun JC, Beilke JN, Lanier LL (2009) Adaptive immune features of natural killer cells. *Nature* 457(7229):557–561.
5. Nabekura T, et al. (2014) Costimulatory molecule DNAM-1 is essential for optimal differentiation of memory natural killer cells during mouse cytomegalovirus infection. *Immunity* 40(2):225–234.
6. Sun JC, et al. (2012) Proinflammatory cytokine signaling required for the generation of natural killer cell memory. *J Exp Med* 209(5):947–954.
7. Orr MT, et al. (2009) Ly49H signaling through DAP10 is essential for optimal natural killer cell responses to mouse cytomegalovirus infection. *J Exp Med* 206(4):807–817.
8. Nabekura T, Girard J-P, Lanier LL (2015) IL-33 receptor ST2 amplifies the expansion of NK cells and enhances host defense during mouse cytomegalovirus infection. *J Immunol* 194(12):5948–5952.
9. Madera S, Sun JC (2015) Cutting edge: Stage-specific requirement of IL-18 for antiviral NK cell expansion. *J Immunol* 194(4):1408–1412.
10. Orange JS, Wang B, Terhorst C, Biron CA (1995) Requirement for natural killer cell-produced interferon gamma in defense against murine cytomegalovirus infection and enhancement of this defense pathway by interleukin 12 administration. *J Exp Med* 182(4):1045–1056.
11. Vivier E, et al. (2011) Innate or adaptive immunity? The example of natural killer cells. *Science* 331(6013):44–49.
12. Devergne O, et al. (1996) A novel interleukin-12 p40-related protein induced by latent Epstein-Barr virus infection in B lymphocytes. *J Virol* 70(2):1143–1153.
13. Collison LW, et al. (2007) The inhibitory cytokine IL-35 contributes to regulatory T-cell function. *Nature* 450(7169):566–569.
14. Wang R-X, et al. (2014) Interleukin-35 induces regulatory B cells that suppress autoimmune disease. *Nat Med* 20(6):633–641.
15. Wirtz S, et al. (2005) EBV-induced gene 3 transcription is induced by TLR signaling in primary dendritic cells via NF-kappa B activation. *J Immunol* 174(5):2814–2824.
16. Vignali DAA, Kuchroo VK (2012) IL-12 family cytokines: Immunological playmakers. *Nat Immunol* 13(8):722–728.
17. Pflanz S, et al. (2002) IL-27, a heterodimeric cytokine composed of EBI3 and p28 protein, induces proliferation of naive CD4+ T cells. *Immunity* 16(6):779–790.
18. Awasthi A, et al. (2007) A dominant function for interleukin 27 in generating interleukin 10-producing anti-inflammatory T cells. *Nat Immunol* 8(12):1380–1389.
19. Stumhofer JS, et al. (2007) Interleukins 27 and 6 induce STAT3-mediated T cell production of interleukin 10. *Nat Immunol* 8(12):1363–1371.
20. Robertson MJ (2002) Role of chemokines in the biology of natural killer cells. *J Leukoc Biol* 71(2):173–183.
21. Eischen CM, Schilling JD, Lynch DH, Krammer PH, Leibson PJ (1996) Fc receptor-induced expression of Fas ligand on activated NK cells facilitates cell-mediated cytotoxicity and subsequent autocrine NK cell apoptosis. *J Immunol* 156(8):2693–2699.
22. Campbell AR, et al. (2015) Gene expression profiling of the human natural killer cell response to Fc receptor activation: Unique enhancement in the presence of interleukin-12. *BMC Med Genomics* 8:66.
23. Nieuwenhuis EES, et al. (2002) Disruption of T helper 2-immune responses in Epstein-Barr virus-induced gene 3-deficient mice. *Proc Natl Acad Sci USA* 99(26):16951–16956.
24. Campbell ID, Spitzfaden C (1994) Building proteins with fibronectin type III modules. *Structure* 2(5):333–337.
25. Stack G, Stacey MA, Humphreys IR (2012) Herpesvirus exploitation of host immune inhibitory pathways. *Viruses* 4(8):1182–1201.
26. Mandaric S, et al. (2012) IL-10 suppression of NK/DC crosstalk leads to poor priming of MCMV-specific CD4 T cells and prolonged MCMV persistence. *PLoS Pathog* 8(8):e1002846.
27. Lee S-H, Kim K-S, Fodil-Cornu N, Vidal SM, Biron CA (2009) Activating receptors promote NK cell expansion for maintenance, IL-10 production, and CD8 T cell regulation during viral infection. *J Exp Med* 206(10):2235–2251.
28. Tarrio ML, et al. (2014) Proliferation conditions promote intrinsic changes in NK cells for an IL-10 response. *J Immunol* 193(1):354–363.
29. Humphreys IR, et al. (2007) Cytomegalovirus exploits IL-10-mediated immune regulation in the salivary glands. *J Exp Med* 204(5):1217–1225.
30. Kim D, et al. (2013) TopHat2: Accurate alignment of transcriptomes in the presence of insertions, deletions and gene fusions. *Genome Biol* 14(4):R36.
31. Dillies M-A, et al.; French StatOmique Consortium (2013) A comprehensive evaluation of normalization methods for Illumina high-throughput RNA sequencing data analysis. *Brief Bioinform* 14(6):671–683.
32. Culhane AC, Thioulouse J, Perrière G, Higgins DG (2005) MADE4: An R package for multivariate analysis of gene expression data. *Bioinformatics* 21(11):2789–2790.

Supporting Information

Jensen et al. 10.1073/pnas.1700231114

SI Materials and Methods

Mice and MCMV Infection. WT and EBI3-deficient (B6.129 × $1^{Ebi3tm1Rsb/J}$) mice on a C57BL/6 background were maintained. Mice between 7–10 wk of age were infected with 10^4 pfu of the MCMV Smith strain by intraperitoneal injection.

Cells. The KIR2DS1$^+$ NKL cells were generated by stable transduction of the human NK cell line, NKL, with a pMxs-puro retroviral vector containing cDNA of human KIR2DS1 (GenBank accession no. X89892), a kind gift from Roberto Biassoni, Istituto Giannina Gaslini, Genoa, Italy. The KIR2DS1$^+$ NKL cells were selected with puromycin and subsequently sorted to generate a homogenous KIR2DS1-expressing cell line. The Ly49H$^+$ NKL cells were generated by stable transduction of NKL cells with a pMX retroviral vector, a kind gift from Hisashi Arase, Osaka University, Osaka, containing cDNA of the mouse B6 allele of *Klra8* (GenBank accession no. U12889). The Ly49H$^+$ NKL cells were single-cell–cloned to generate a homogenous Ly49H-expressing cell line. NKL cells were maintained in RPMI-1640 medium (Corning Cellgro, Mediatech Inc.) containing 10% (vol/vol) FBS (Thermo Scientific), 2 mM L-glutamine (UCSF cell culture facility), and penicillin (100 IU/mL) and streptomycin (100 μg/mL) (Corning Cellgro), supplemented with 200 U/mL human IL-2 (generously provided by Prometheus Laboratories, Inc.). PBMCs were isolated from blood obtained from the Stanford Blood Center or the Blood Centers of the Pacific by density gradient centrifugation using Ficoll-Paque PLUS (GE Healthcare Bio-Sciences AB). NK cells were purified from PBMCs using an NK cell isolation kit (Miltenyi Biotec GmbH) (>90% purity) or by sorting CD3$^-$CD56$^+$ NK cells (>99% purity). The primary human NK cells were cultured in RPMI-1640 medium containing 10% FBS, 2 mM L-glutamine, penicillin, and streptomycin.

In Vitro Stimulation of NKL Cells and Primary Human NK Cells.

Plate-bound Ab stimulations. Nunc maxisorp ELISA plates (Thermo Fisher Scientific) were washed twice in PBS and then coated with 1 μg/mL anti-NKG2D mAb (149810, R&D Systems), 5 μg/mL anti-NKG2D mAb (1D11, BioLegend), 5 μg/mL anti-KIR2D mAb (clone HP3E4, BD Biosciences), 5 μg/mL anti-Ly49H (3D10, eBioscience), 1 or 5 μg/mL control mouse IgG_1 (MOPC-21, UCSF Monoclonal Antibody Core), or 5 μg/mL control mouse IgM (11E10, eBioscience) in PBS for 24 h at 4 °C. The ELISA plates were washed twice in PBS and blocked in complete culture medium for 10 min at room temperature (RT) before 150,000 cells were added to each well in the ELISA plate. NKL cells were stimulated with control IgG_1, control IgM, anti-NKG2D, anti-KIR2D, or anti-Ly49H plate-bound mAb for 4 h or 18 h (for deep sequencing) or for 24 h (for flow cytometry and Western blot analysis) at 37 °C and 5% CO_2. Primary human NK cells were primed in 200 U/mL human IL-2 for 24 h and then stimulated with plate-bound control IgG_1 or anti-NKG2D mAb for 24 h (flow cytometry) at 37 °C and 5% CO_2.

Cytokine stimulations. NKL cells and primary human NK cells were stimulated with 20 ng/mL human IL-18 (R&D Systems) and/or 10 ng/mL human IL-12 (R&D Systems) for 24 h (for flow cytometry and Western blot analysis) at 37 °C and 5% CO_2. For the EBI3, p35, and p28 measurements by flow cytometry, GolgiSTOP and GolgiPLUG (BD Bioscience, final dilution 1:1,500 and 1:1,000, respectively) were added for the last 4 h (NKL cells) or 6 h (primary human NK cells) of stimulation.

Real-Time PCR. For MCMV quantification, oral lavage was collected by washing the mouse sublingual cavity with sterile saline, and 1-μL samples were used for quantitative PCR (qPCR) analysis. DNA was isolated from peripheral blood and homogenates of salivary glands by using a ReliaPrep Blood gDNA Miniprep System kit (Promega), and 1-μL samples were used for qPCR analysis. The relative copy numbers of MCMV IE1 were determined by quantitative PCR analysis with SYBR green master mix reagent (Invitrogen) using standard conditions and the following primer pair: MCMV-IE1_Forward—5′-AGCCACCAACATT-GACCACGCAC-3′ and MCMV-IE1_Reverse—5′-GCCCC-AACCAGGACA CACAACTC-3′. Mice were monitored daily for weight loss and survival.

Flow Cytometry. The mAbs used for cell-surface staining were the following: FITC-conjugated anti-mouse MHC class II (M5/114.15.2, eBioscience); FITC-conjugated anti-Ly49D (4E5, BioLegend); FITC-conjugated anti-mouse NKG2A,C,E (20d5, eBioscience); FITC-conjugated anti-mouse CD69 (HI.2F3, BD Biosciences); FITC- or PE-conjugated anti-Ly49H (3D10, BioLegend); PE-conjugated anti-mouse CD27 (M-T271, BioLegend); PE-conjugated anti-mouse NKp46 (29A1.4, BioLegend); PE-conjugated anti-mouse NKG2D (CX5, eBioscience); PE-conjugated anti-mouse CD86 (GL1, BioLegend); PE-conjugated anti-mouse NKG2D (CX5, eBioscience); PE-conjugated anti-mouse gp130 (4H1B35, BioLegend); PE-conjugated anti-human gp130 (2E1B02, BioLegend); APC-conjugated anti-mouse CD11b (M1/70, BioLegend); APC-conjugated anti-mouse CD40 (3/23, BioLegend); APC-conjugated anti-mouse KLRG1 (2FI/KLRG1, BioLegend); APC-conjugated anti-human and -mouse IL-12Rβ2 (305719, R&D Systems); APC-conjugated anti-human KIR2DL1/DS1 (11PB6, Miltenyi Biotec); APC-conjugated anti-human NKG2D (149810, R&D Systems); PerCP-Cy5.5-conjugated anti-mouse NK1.1 (PK136, BioLegend); PerCP-Cy5.5-conjugated anti-human CD56 (HCD56, BioLegend); AF700-conjugated anti-mouse TCRβ (H57-597, BioLegend); AF700-conjugated anti-human CD3 (HIT3a, BioLegend); PE-Cy7–conjugated anti-mouse CD11c (HL3, BD Biosciences); PE-Cy7–conjugated anti-mouse TCRβ (H57-597, BioLegend); APC-Cy7-conjugated anti-mouse TCRβ (H57-597, BioLegend); vF421-conjugated anti-mouse CD8 (53-6.7, Tonbo Biosciences); PB-conjugated anti-Ly49A (A1/Ly49A, BioLegend); and PB-conjugated anti-B220 (R43-6B2, BioLegend). The mAbs used for intracellular staining werethe following: eFlour660-conjugated anti-human p28 (3D1p28, eBioscience); PE-conjugate anti-human EBI3 (B032F6, BioLegend); APC-conjugated anti-human and mouse p35 (27537, R&D Systems); APC-conjugated anti-human and mouse IL-12Rβ2; APC-conjugated anti-mouse IFNγ (XMG1.2, BioLegend); PE-conjugated anti-mouse IL-10 (JES5-16E3, BioLegend); PE-conjugated anti-mouse EBI3 (355022, R&D Systems); AF647-conjugated anti-mouse p28 (516903, BioLegend). For surface staining, cells were incubated with the indicated mAbs or isotype-matched control antibodies (Jackson ImmunoResearch, BD Biosciences, eBioscience, or BioLegend) for 20 min on ice. When applicable, mouse Fc receptors were blocked with anti-CD16 + CD32 mAb 2.4G2 before staining. When indicated, NKL cells were stained by incubating the cells with mAbs for 1 h at 37 °C with 5% CO_2. For intracellular staining, cells were fixed and permeabilized using the Cytofix/Cytoperm kit (BD Biosciences) according to the manufacturer's protocol and subsequently stained with the indicated mAbs or isotype-matched control antibodies (BD Biosciences, eBioscience, or BioLegend) for either 20 min on ice or 30 min at RT. Samples were acquired on a LSRII (BD Biosciences) and analyzed with FlowJo software (Tree Star). Live single cells were gated based

on forward (Fsc) and side light-scatter (Ssc) profiles. Human NK cells were gated as $CD3^{-}CD56^{+}$ cells. Mouse NK cells, B cells, T cells, and DCs were gated as $TCR\beta^{-}$ $NK1.1^{+}$ cells, $TCR\beta^{-}$ $B220^{+}$ cells, $TCR\beta^{+}$ $NK1.1^{-}$ cells, and $TCR\beta^{-}NK1.1^{-}B220^{-}$MHC class II^{+} $CD11c^{hi}$ cells, respectively.

IL-10 ELISA. Blood was obtained from MCMV-infected (day 5) and noninfected control mice by cardiac puncture and was allowed to clot in serum separator tubes for 30 min at RT. Sera were collected after centrifugation (13,000 × *g* for 10 min at RT) and the IL-10 concentration was determined using an OptEIA Mouse IL-10 ELISA kit (BD Biosciences) according to the manufacturer's instructions.

Western Blot Analysis. Supernatants from stimulated NKL cells were concentrated 10× using 10K Amicon Ultra centrifugal filters (Millipore). The supernatants for p35 Western blot analysis were precleared with goat anti-mouse IgG Dynabeads by rotating for 30 min at 4 °C, and the Dynabeads were removed by magnet before concentration. The concentrated supernatants were then diluted in RIPA buffer (150 mM NaCl, 1% Nonidet P-40, 0.5% sodium deoxycholate, 0.1% SDS, 50 mM Tris, pH 8), and the samples were incubated at 70 °C for 10 min in NuPAGE SDS Sample Buffer (Life Technologies) containing NuPAGE Reducing Agent (Life Technologies). Proteins were separated on a 4–12% Bis–Tris NuPAGE gel (Life Technologies) in MES or MOPS NuPAGE Running Buffer (Life Technologies) containing NuPAGE Antioxidant (Life Technologies) at 200 V for 90 min at 4 °C. Human recombinant EBI3 (ab83026, Abcam) or human recombinant IL-12 (R&D Systems) was included as positive control. Samples were transferred to Immobilon PVDF membranes (Millipore) in NuPAGE transfer buffer (Life Technologies) containing NuPAGE antioxidant and 10% methanol for 1 h at 20 V at RT and blocked in 5% milk in Tris-buffered saline with Tween 20 (TBST) buffer (0.01 M Tris, pH 8, 0.15 M NaCl, 0.5% Tween-20) for 1 h at RT. Membranes were probed with rabbit anti-human EBI3 polyclonal antibody (H-110, Santa Cruz Biotechnology, 1:400 dilution) or mouse anti-human/mouse IL-12/IL-35 p35 monoclonal Ab (27537, R&D Systems, 1:500 dilution) in TBST + 2% BSA+ 0.05% azide buffer overnight at 4 °C, followed by incubation with HRP-conjugated goat anti-rabbit IgG (Jackson ImmunoResearch) or HRP-conjugated donkey anti-mouse IgG (Jackson ImmunoResearch) in TBST + 2% BSA buffer) for 1 h at RT and then visualized by using the Amersham ECL Prime WB detection reagent (GE Healthcare). The mean intensity of the bands was calculated using Photoshop by subtracting the histogram mean for the background from the mean obtained for each sample.

Deep Sequencing. Total RNA was isolated from NKL cells stimulated with plate-bound Ab for 4 h or 18 h using an RNeasy Kit (Qiagen). Libraries were constructed according to standard Illumina protocols. The integrity and quality of RNA and cDNA were monitored by using an Agilent Bioanalyzer 2100. Ultrahigh-throughput sequencing was performed on the Illumina HiSeq for 2 × 100-bp paired-end reads. Fastqc was used for read quality control, and fastq quality filter (-q 30 -p 85) and fastq quality trimmer (-t 30 -l 40) were used for read filtering. All reads where then aligned with tophat2 and the GRCh37_r69 human reference genome, using the default setting except for allowing segment-mismatches (2), segment-length (25), and mate-std-dev (395) (30). Read counts were obtained with Htseq running in intersection-nonempty mode. Read counts where normalized using the calcNormFactors function of the edgeR software package together with log2 transformation. Comparative analysis was performed using linear models on these normalized values as recommended by Dillies et al. (31). The individual datasets represent independent experiments with NKL cells. The GSEA was performed using the online analysis tool DAVID (version 6.7) together with all gene sets from the Gene Ontology (GOTERM_MF_FAT definition).

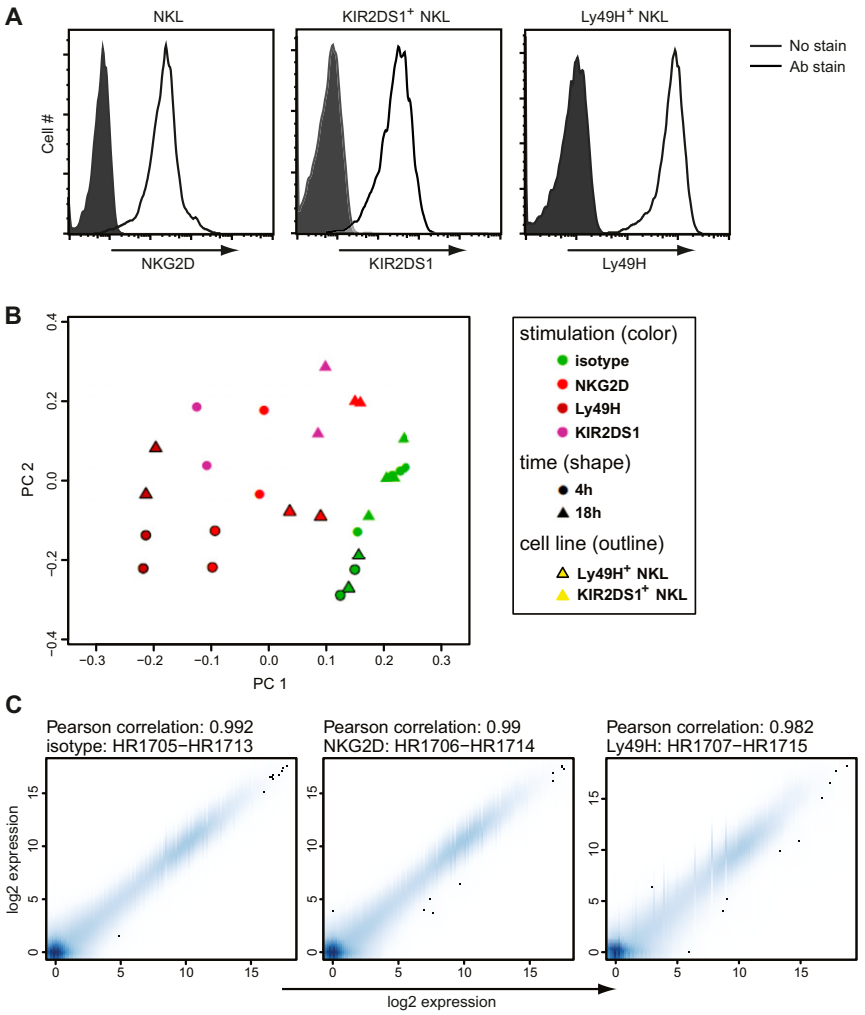

Fig. S1. (*A*) NKG2D, KIR2DS1, and Ly49H cell-surface expression of transduced NKL cells was verified by flow cytometry. (*B*) The PCA plot was generated using the Bioconductor package made4 (version 1.40.0) (32) and calculated after removing nonexpressed genes and scaling the log2 expression values to 0 mean and unit variance. (*C*) The replicate plots were calculated as Pearson correlations of the log2 expression values of all measured genes and plotted using the smoothScatter function of R. (*B* and *C*) The individual datasets represent independent experiments with NKL cells.

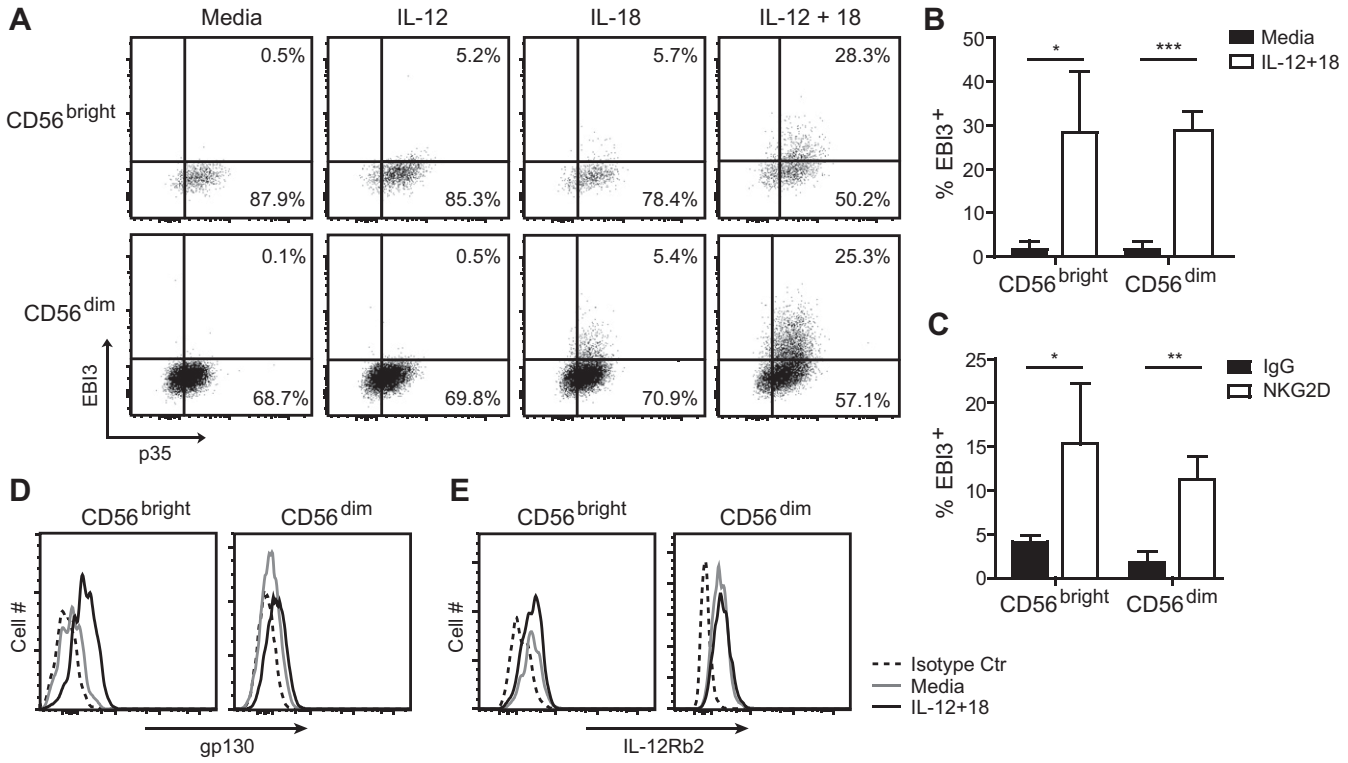

Fig. S2. EBI3 and gp130 protein expression is increased in human primary NK cells in response to receptor- and cytokine-mediated stimulation. Human primary CD56^{bright} and CD56^{dim} NK cells were isolated from blood obtained from healthy blood donors and (*A*, *B*, *D*, and *E*) either left unstimulated or stimulated with IL-12 and/or IL-18 for 24 h or (*C*) primed with IL-2 for 24 h before being stimulated with plate-bound isotype-matched control Ig or anti-NKG2D mAb for 24 h. (*A*–*C*) Intracellular EBI3 and p35 protein expression was analyzed by flow cytometry. (*A*) Data are representative of three different donors. (*B* and *C*) Data show mean ± SD from three different donors. (*D*) Surface gp130 expression and (*E*) intracellular IL-12Rβ2 expression was examined by flow cytometry. Data are representative of three different donors. Statistical analysis was performed by two-tailed unpaired Student's *t* test (*$P < 0.05$, **$P < 0.01$, and ***$P < 0.001$).

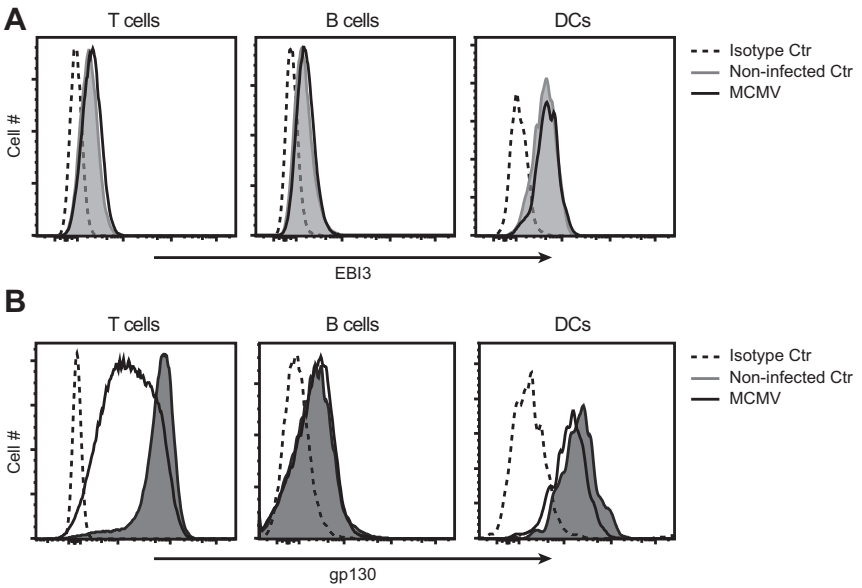

Fig. S3. (*A*) Intracellular EBI3 protein expression was examined by flow cytometry in splenic T cells, B cells, and DCs from noninfected and MCMV-infected (day 2.5) WT B6 mice. (*B*) gp130 surface expression was examined by flow cytometry in splenic T cells, B cells, and DCs from noninfected and MCMV-infected (day 2) WT B6 mice. (*A* and *B*) Data are representative of four or six mice from two independent experiments.

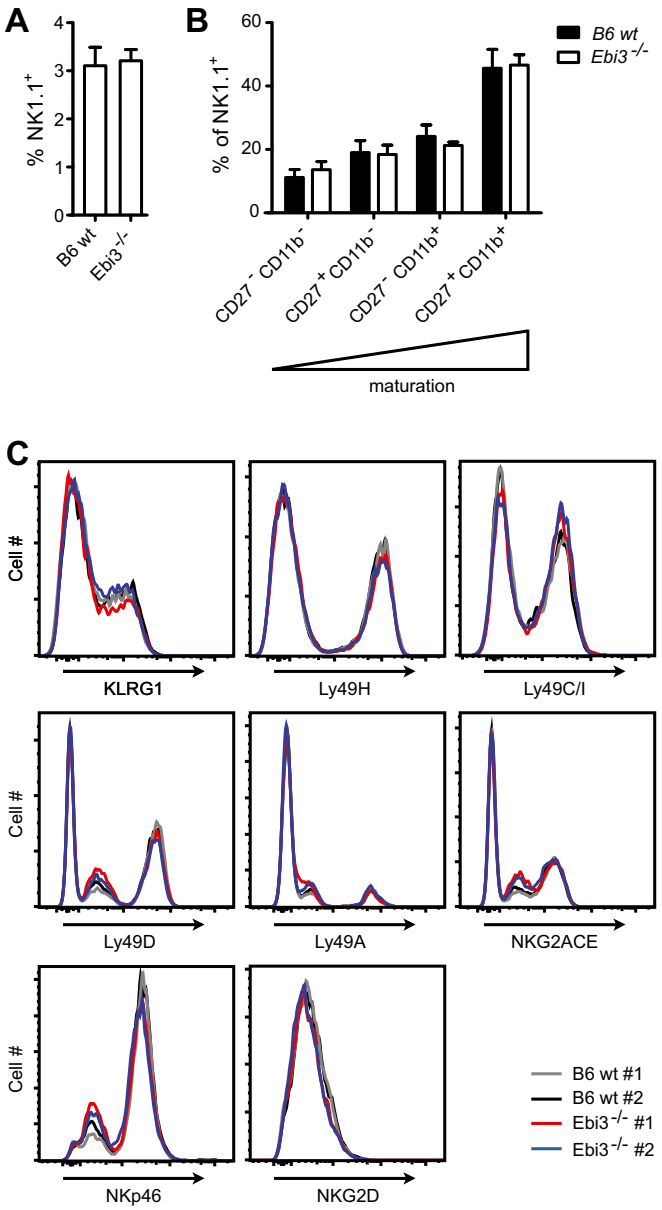

Fig. S4. (*A*) The percentage of splenic TCRβ$^-$ NK1.1$^+$ cells and (*B*) the maturation stages from WT and *Ebi3*$^{-/-}$ B6 mice were examined by flow cytometry. $n = 5$ for each mouse strain from two independent experiments. Data show mean ± SD. (*C*) Surface levels of the indicated NK cell receptors on splenic TCRβ$^-$ NK1.1$^+$ cells from WT and *Ebi3*$^{-/-}$ B6 mice were examined by flow cytometry. Data shown are from two mice from each strain and are representative of five mice from two independent experiments.

Dataset S1. Deep-sequencing data

Dataset S1

The dataset includes all genes with an average fold-change of at least 1.5 between the receptor-stimulated and control-treated NKL cells. Shown are the ensemble ID, gene symbol, fold-change, and *P* value for the involved receptor stimulations.

Dataset S1

Specific genes for NKG2D_4h stimulation:

Ensembl ID	Gene symbol	Fold change (NKG2D_4h)	p-value (NKG2D_4h)
ENSG00000262304	TRPV1 (ion channel)	2.87	0.00197
ENSG00000251279	CTC-436P18.1 (unknown)	2.77	0.0136
ENSG00000179256	SMCO3 (membrane protein)	1.82	0.0317
ENSG00000206989	SNORD63 (ncRNA)	1.75	0.00254

Specific genes for KIR2DS1_4h stimulation:

Ensembl ID	Gene symbol	Fold change (KIR2DS1_4h)	p-value (KIR2DS1_4h)
ENSG00000185433	LINC00158	2.88	6.62E-14
ENSG00000112182	BACH2	2.71	0.0064
ENSG00000126010	GRPR	2.57	0.0316
ENSG00000179059	ZFP42	2.53	0.004
ENSG00000166292	TMEM100	2.46	5.69E-7
ENSG00000175866	BAIAP2	2.38	0.0198
ENSG00000140511	HAPLN3	2.32	0.0207
ENSG00000115594	IL1R1	2.19	4.41E-14
ENSG00000008283	CYB561	2.07	5.08E-21
ENSG00000154479	CCDC173	2.03	0.00251
ENSG00000256128	LINC00944	2.00	0.0155
ENSG00000160789	LMNA	2.00	5.51E-7
ENSG00000130396	MLLT4	1.96	0.019
ENSG00000080618	CPB2	1.93	0.0113
ENSG00000251230	LOC731424	1.88	0.00303
ENSG00000189190	ZNF600	1.88	0.00251
ENSG00000182568	SATB1	1.77	9.29E-4
ENSG00000080823	MOK	1.76	3.6E-12
ENSG00000128965	CHAC1	1.74	2.31E-14
ENSG00000111837	MAK	1.71	2.85E-13
ENSG00000164683	HEY1	1.69	8.3E-5
ENSG00000150347	ARID5B	1.69	3.66E-55
ENSG00000121594	CD80	1.68	3.1E-33
ENSG00000250295	LOC101926926	1.64	0.0156
ENSG00000169248	CXCL11	1.59	0.0114
ENSG00000167703	SLC43A2	1.59	5.2E-10
ENSG00000100583	SAMD15	1.59	1.04E-4
ENSG00000105499	PLA2G4C	1.56	0.0125
ENSG00000118495	PLAGL1	1.55	3.24E-10
ENSG00000225439	BOLA3-AS1	1.55	0.014
ENSG00000137216	TMEM63B	1.55	8.56E-28
ENSG00000106089	STX1A	1.54	1.87E-11
ENSG00000104998	IL27RA	1.53	4.91E-29
ENSG00000081985	IL12RB2	1.50	2.68E-38
ENSG00000136158	SPRY2	1.50	0.0235
ENSG00000168016	TRANK1	-1.50	3.6E-7
ENSG00000091592	NLRP1	-1.50	2.32E-6
ENSG00000177674	AGTRAP	-1.51	0.00775
ENSG00000241316	SUCLG2-AS1	-1.52	0.0389
ENSG00000145246	ATP10D	-1.53	1.15E-7
ENSG00000136531	SCN2A	-1.53	0.0462
ENSG00000182257	PRR34	-1.54	0.0166
ENSG00000183682	BMP8A	-1.66	0.0199
ENSG00000162739	SLAMF6	-1.66	2.25E-6
ENSG00000198796	ALPK2	-1.68	0.0104
ENSG00000135063	FAM189A2	-1.72	2.24E-4
ENSG00000174600	CMKLR1	-1.73	1.64E-6
ENSG00000112812	PRSS16	-1.80	0.00387
ENSG00000006468	ETV1	-1.85	0.0107
ENSG00000170858	LILRP2	-1.86	1.62E-9
ENSG00000173269	MMRN2	-1.90	0.0417
ENSG00000129422	MTUS1	-1.96	0.0166
ENSG00000188869	TMC3	-2.11	0.037
ENSG00000137831	UACA	-2.27	2.83E-12
ENSG00000205821	LOC284009	-2.43	0.00594
ENSG00000181903	OR4C6	-2.49	3.88E-4
ENSG00000110169	HPX	-2.53	0.0386

ENSG00000212658	KRTAP29-1	-3.13	0.0407
ENSG00000114993	RTKN	-5.12	0.0485
ENSG00000234906	APOC2	-5.27	0.0262
ENSG00000118473	SGIP1	-5.99	3.41E-4

Specific genes for Ly49H_4h stimulation:

Ensembl ID	**Gene symbol**	**Fold change (Ly49H_4h)**	**p-value (Ly49H_4h)**
ENSG00000102962	CCL22	6.45	7.31E-9
ENSG00000166670	MMP10	6.45	7.31E-9
ENSG00000126549	STATH	6.18	4.3E-18
ENSG00000115009	CCL20	6.10	3.3E-7
ENSG00000169194	IL13	5.79	9.98E-18
ENSG00000126259	KIRREL2	5.75	1.1E-12
ENSG00000138798	EGF	5.69	2.44E-5
ENSG00000197632	SERPINB2	5.47	3.49E-8
ENSG00000136695	IL36RN	4.95	0.0047
ENSG00000254997	KRTAP5-9	4.95	0.0047
ENSG00000149256	TENM4	4.95	0.0047
ENSG00000188800	TMCO2	4.84	0.0303
ENSG00000262202	SNORD3D	4.73	0.0124
ENSG00000168348	INSM2	4.62	3.39E-5
ENSG00000260151	LOC101929180	4.51	0.0477
ENSG00000224675	LOC100144595	4.47	0.0344
ENSG00000162892	IL24	4.14	6.36E-11
ENSG00000251191	LINC00589	4.09	0.00312
ENSG00000157680	DGKI	4.05	1.59E-6
ENSG00000233397	LOC100506077	3.95	0.00528
ENSG00000222040	ADRA2B	3.92	0.00752
ENSG00000141574	SECTM1	3.91	0.00754
ENSG00000102024	PLS3	3.81	2.83E-5
ENSG00000075891	PAX2	3.72	0.0205
ENSG00000131203	IDO1	3.7	0.0283
ENSG00000072682	P4HA2	3.52	0.0476
ENSG00000237330	RNF223	3.49	0.0481
ENSG00000253102	LRRC59	3.48	0.00983
ENSG00000140538	NTRK3	3.43	0.00887
ENSG00000234336	JAZF1-AS1	3.32	3.54E-7
ENSG00000205863	C1QTNF9B	3.27	0.0217
ENSG00000258946	LOC100506446	3.18	0.00106
ENSG00000175003	SLC22A1	3.18	0.00104
ENSG00000060558	GNA15	3.02	0.00116
ENSG00000261671	LOC100130992	3.01	0.0126
ENSG00000243004	LOC101927668	2.83	8.54E-5
ENSG00000173451	THAP2	2.77	1.79E-27
ENSG00000139572	GPR84	2.76	0.00379
ENSG00000257242	C12orf79	2.74	0.000744
ENSG00000162510	MATN1	2.71	5.74E-13
ENSG00000140287	HDC	2.71	3.26E-25
ENSG00000226396	RPS14P3	2.69	4.57E-7
ENSG00000203837	PNLIPRP3	2.61	0.0322
ENSG00000041982	TNC	2.61	1.6E-36
ENSG00000153093	ACOXL	2.58	0.00344
ENSG00000161270	NPHS1	2.56	1.47E-4
ENSG00000188783	PRELP	2.53	0.0195
ENSG00000131711	MAP1B	2.52	0.0383
ENSG00000214900	C14orf182	2.5	2.23E-20
ENSG00000186652	PRG2	2.48	0.00601
ENSG00000115956	PLEK	2.48	2.61E-44
ENSG00000141316	SPACA3	2.45	4.32E-12
ENSG00000156127	BATF	2.41	1.94E-22
ENSG00000136634	IL10	2.4	6.47E-17
ENSG00000222041	LINC00152	2.39	2.7E-18
ENSG00000265452	MIR3682	2.36	5.44E-6
ENSG00000243795	LOC101929717	2.35	0.0307
ENSG00000221955	SLC12A8	2.34	0.0296
ENSG00000248334	WHAMMP2	2.33	9.0E-17
ENSG00000117090	SLAMF1	2.33	4.66E-33
ENSG00000261105	LMO7-AS1	2.31	2.42E-4
ENSG00000197249	SERPINA1	2.29	0.00162
ENSG00000067177	PHKA1	2.25	1.12E-4

ENSG00000226009	KCNIP2-AS1	2.25	2.46E-5
ENSG00000212607	SNORA45B	2.25	4.32E-7
ENSG00000232533	LOC100507507	2.22	2.56E-15
ENSG00000175592	FOSL1	2.21	5.69E-21
ENSG00000260372	AQP4-AS1	2.2	0.00773
ENSG00000174500	GCSAM	2.18	0.0238
ENSG00000186827	TNFRSF4	2.18	2.05E-12
ENSG00000258586	LOC100506498	2.17	2.44E-6
ENSG00000178690	DYNAP	2.16	0.00657
ENSG00000231105	LOC100506801	2.15	2.77E-5
ENSG00000196843	ARID5A	2.14	1.41E-11
ENSG00000106537	TSPAN13	2.13	5.84E-4
ENSG00000230641	USP12-AS2	2.11	0.00608
ENSG00000196436	NPIPB15 (includes others)	2.09	1.6E-8
ENSG00000234263	LOC101928461	2.07	0.0357
ENSG00000229891	LINC01315	2.07	0.00361
ENSG00000172965	MIR4435-1HG	2.07	6.25E-13
ENSG00000133639	BTG1	2.07	4.02E-35
ENSG00000266040	LOC101929533	2.06	0.0253
ENSG00000169413	RNASE6	2.06	0.00379
ENSG00000102265	TIMP1	2.06	2.01E-15
ENSG00000248099	INSL3	2.04	7.05E-4
ENSG00000111729	CLEC4A	2.04	1.27E-4
ENSG00000182368	FAM27C	2.03	0.00213
ENSG00000145777	TSLP	2.03	4.07E-6
ENSG00000236719	OVAAL	2.03	4.14E-7
ENSG00000137648	TMPRSS4	2.02	0.00165
ENSG00000187984	ANKRD19P	2.02	2.07E-4
ENSG00000172183	ISG20	1.96	2.07E-8
ENSG00000122862	SRGN	1.96	8.34E-30
ENSG00000168878	SFTPB	1.94	0.0197
ENSG00000185507	IRF7	1.94	3.19E-23
ENSG00000100450	GZMH	1.93	1.87E-4
ENSG00000229056	LOC101927482	1.93	6.2E-8
ENSG00000131015	ULBP2	1.93	5.72E-28
ENSG00000143153	ATP1B1	1.92	2.08E-6
ENSG00000161912	ADCY10P1	1.92	1.49E-6
ENSG00000100292	HMOX1	1.92	5.1E-7
ENSG00000186132	C2orf76	1.92	4.92E-16
ENSG00000060642	PIGV	1.91	2.98E-21
ENSG00000267532	MIR497HG	1.89	7.6E-4
ENSG00000207501	RNVU1-14	1.89	1.69E-4
ENSG00000116285	ERRFI1	1.88	0.0357
ENSG00000255198	SNHG9	1.88	4.18E-7
ENSG00000161326	DUSP14	1.88	1.03E-17
ENSG00000116717	GADD45A	1.88	5.28E-35
ENSG00000171522	PTGER4	1.88	2.01E-36
ENSG00000100276	RASL10A	1.87	0.00411
ENSG00000196329	GIMAP5	1.87	1.04E-9
ENSG00000257704	INAFM1	1.86	9.0E-9
ENSG00000196569	LAMA2	1.85	7.67E-5
ENSG00000107968	MAP3K8	1.85	3.37E-24
ENSG00000137575	SDCBP	1.85	2.02E-39
ENSG00000155428	TRIM73/TRIM74	1.84	0.029
ENSG00000207205	RNVU1-15	1.82	0.0184
ENSG00000207166	SNORA68	1.82	4.73E-5
ENSG00000173812	EIF1	1.82	7.19E-21
ENSG00000234618	RPSAP9	1.81	1.97E-7
ENSG00000267226	LOC101927322	1.80	0.00238
ENSG00000185499	MUC1	1.80	4.8E-11
ENSG00000228486	LINC01125	1.79	5.07E-10
ENSG00000181773	GPR3	1.79	1.05E-12
ENSG00000136560	TANK	1.79	4.46E-24
ENSG00000169246	NPIPB4 (includes others)	1.78	2.8E-7
ENSG00000160888	IER2	1.78	3.74E-21
ENSG00000164850	GPER1	1.77	0.00587
ENSG00000136205	TNS3	1.77	0.00128
ENSG00000237541	HLA-DQA2	1.77	1.07E-5
ENSG00000173846	PLK3	1.77	1.13E-20
ENSG00000224420	ADM5	1.76	5.0E-8
ENSG00000166401	SERPINB8	1.76	3.68E-11

ENSG00000186010	NDUFA13	1.75	5.85E-8
ENSG00000027869	SH2D2A	1.75	1.32E-12
ENSG00000121039	RDH10	1.75	3.11E-33
ENSG00000142227	EMP3	1.72	1.59E-12
ENSG00000257027	LOC101928054	1.71	4.27E-17
ENSG00000118785	SPP1	1.71	2.76E-19
ENSG00000103642	LACTB	1.71	1.31E-23
ENSG00000145365	TIFA	1.71	7.16E-24
ENSG00000240567	LOC101243545	1.70	5.09E-5
ENSG00000227373	LOC102724601	1.69	0.00601
ENSG00000172653	HEATR9	1.68	1.45E-4
ENSG00000102096	PIM2	1.66	3.69E-15
ENSG00000099985	OSM	1.66	3.46E-25
ENSG00000151715	TMEM45B	1.64	0.00339
ENSG00000221539	SNORD99	1.64	2.32E-4
ENSG00000187944	C2orf66	1.63	5.12E-7
ENSG00000230055	CISD3	1.63	1.39E-8
ENSG00000177105	RHOG	1.63	4.03E-16
ENSG00000214435	AS3MT	1.62	0.00243
ENSG00000171159	C9orf16	1.62	1.09E-6
ENSG00000125462	C1orf61	1.62	3.04E-8
ENSG00000151929	BAG3	1.62	1.64E-13
ENSG00000140830	TXNL4B	1.62	1.48E-13
ENSG00000115919	KYNU	1.62	7.41E-14
ENSG00000135740	SLC9A5	1.62	2.74E-16
ENSG00000242252	BGLAP	1.61	0.00949
ENSG00000187990	HIST1H2BG	1.61	0.00367
ENSG00000110944	IL23A	1.61	1.07E-5
ENSG00000107738	C10orf54	1.61	8.72E-9
ENSG00000141682	PMAIP1	1.61	7.56E-24
ENSG00000220749	RPL21P28	1.60	0.00119
ENSG00000253276	CCDC71L	1.60	4.14E-7
ENSG00000103257	SLC7A5	1.60	9.75E-22
ENSG00000221916	C19orf73	1.59	0.0161
ENSG00000137869	CYP19A1	1.59	0.00358
ENSG00000102393	GLA	1.59	1.09E-11
ENSG00000260583	LINC00515	1.58	0.0244
ENSG00000107175	CREB3	1.58	3.65E-11
ENSG00000104064	GABPB1	1.58	9.22E-25
ENSG00000184260	HIST2H2AC	1.57	0.0247
ENSG00000127666	TICAM1	1.57	1.89E-12
ENSG00000184203	PPP1R2	1.57	4.6E-14
ENSG00000176635	HORMAD2	1.56	0.00825
ENSG00000243449	C4orf48	1.56	0.00049
ENSG00000158050	DUSP2	1.56	2.66E-18
ENSG00000186891	TNFRSF18	1.55	0.00222
ENSG00000237181	LOC101926963	1.55	2.56E-8
ENSG00000018280	SLC11A1	1.54	1.01E-4
ENSG00000177700	POLR2L	1.54	1.07E-5
ENSG00000237819	LOC101927497	1.54	1.88E-7
ENSG00000176845	METRNL	1.54	4.72E-15
ENSG00000091879	ANGPT2	1.53	0.0335
ENSG00000214401	KANSL1-AS1	1.53	1.16E-6
ENSG00000166866	MYO1A	1.52	0.0139
ENSG00000204832	ST8SIA6-AS1	1.52	0.00323
ENSG00000143443	C1orf56	1.52	6.11E-4
ENSG00000108639	SYNGR2	1.52	6.11E-17
ENSG00000105472	CLEC11A	1.51	7.41E-4
ENSG00000173559	NABP1	1.51	1.39E-15
ENSG00000120129	DUSP1	1.51	2.41E-17
ENSG00000204386	NEU1	1.50	8.22E-16
ENSG00000126860	EVI2A	1.50	8.8E-21
ENSG00000168884	TNIP2	1.50	5.05E-25
ENSG00000181408	UTS2R	-1.50	0.0171
ENSG00000113810	SMC4	-1.51	5.38E-4
ENSG00000076555	ACACB	-1.51	1.68E-5
ENSG00000183542	KLRC4	-1.51	7.93E-8
ENSG00000183508	FAM46C	-1.51	4.89E-15
ENSG00000263408	MIR4453	-1.52	0.0439
ENSG00000246859	STARD4-AS1	-1.52	0.0168
ENSG00000089505	CMTM1	-1.52	0.00228

ENSG00000183625	CCR3	-1.52	1.33E-6
ENSG00000237004	ZNRF2P1	-1.53	4.08E-4
ENSG00000205790	DPP9-AS1	-1.53	2.41E-5
ENSG00000076641	PAG1	-1.53	4.02E-6
ENSG00000111859	NEDD9	-1.53	4.11E-14
ENSG00000172888	ZNF621	-1.54	0.00698
ENSG00000074855	ANO8	-1.54	2.9E-4
ENSG00000127533	F2RL3	-1.54	3.76E-6
ENSG00000226121	AHCTF1P1	-1.55	0.0174
ENSG00000136925	TSTD2	-1.55	0.00215
ENSG00000140632	GLYR1	-1.55	0.00131
ENSG00000254369	HOXA-AS3	-1.56	0.00666
ENSG00000243708	PLA2G4B	-1.56	0.00246
ENSG00000229152	ANKRD10-IT1	-1.57	0.0289
ENSG00000196110	ZNF699	-1.57	0.00302
ENSG00000204131	NHSL2	-1.59	0.00766
ENSG00000235373	LOC100134822	-1.60	0.0249
ENSG00000066230	SLC9A3	-1.60	0.0248
ENSG00000174111	SOCS7	-1.60	7.71E-6
ENSG00000228544	CCDC183-AS1	-1.60	4.69E-6
ENSG00000229325	ACAP2-IT1	-1.61	0.0494
ENSG00000095539	SEMA4G	-1.61	0.00258
ENSG00000260852	FBXL19-AS1	-1.62	8.94E-6
ENSG00000156650	KAT6B	-1.62	3.99E-8
ENSG00000162337	LRP5	-1.64	0.0119
ENSG00000110395	CBL	-1.64	7.64E-4
ENSG00000149503	INCENP	-1.64	2.97E-6
ENSG00000197933	ZNF823	-1.65	0.0235
ENSG00000245648	LOC101928100	-1.65	0.00203
ENSG00000162591	MEGF6	-1.65	7.7E-8
ENSG00000165475	CRYL1	-1.66	0.00169
ENSG00000258659	TRIM34	-1.67	1.54E-4
ENSG00000054793	ATP9A	-1.67	5.84E-6
ENSG00000225373	WASH5P	-1.68	2.59E-4
ENSG00000213204	C6orf165	-1.69	0.0335
ENSG00000181523	SGSH	-1.69	0.00407
ENSG00000205047	KLHDC4	-1.69	3.99E-6
ENSG00000164080	RAD54L2	-1.70	0.0131
ENSG00000171282	BAHCC1	-1.70	1.95E-6
ENSG00000248092	NNT-AS1	-1.71	8.59E-7
ENSG00000185453	C19orf68	-1.71	3.44E-8
ENSG00000240970	RPL23AP64	-1.72	0.00428
ENSG00000167377	ZNF23	-1.72	0.00209
ENSG00000168970	JMJD7-PLA2G4B	-1.72	4.65E-4
ENSG00000126895	AVPR2	-1.73	0.00119
ENSG00000204366	ZBTB12	-1.73	1.82E-8
ENSG00000166359	WDR88	-1.74	3.67E-4
ENSG00000169047	IRS1	-1.74	2.39E-6
ENSG00000231711	LINC00899	-1.74	2.71E-8
ENSG00000185278	ZBTB37	-1.75	5.24E-7
ENSG00000092421	SEMA6A	-1.76	0.05
ENSG00000265806	MIR4292	-1.77	0.00477
ENSG00000232803	SLCO4A1-AS1	-1.77	0.00267
ENSG00000205746	LOC101060429	-1.77	0.00131
ENSG00000180539	C9orf139	-1.77	6.2E-10
ENSG00000156475	PPP2R2B	-1.78	0.0218
ENSG00000160293	VAV2	-1.78	4.53E-4
ENSG00000163823	CCR1	-1.78	2.25E-7
ENSG00000214982	PARGP1	-1.78	1.49E-7
ENSG00000131370	SH3BP5	-1.79	0.00197
ENSG00000078018	MAP2	-1.79	8.63E-6
ENSG00000262227	LOC101927979	-1.80	0.00359
ENSG00000223509	WHAMMP1	-1.80	1.51E-4
ENSG00000139194	RBP5	-1.81	0.00363
ENSG00000233122	CTAGE7P	-1.81	0.00209
ENSG00000152402	GUCY1A2	-1.82	0.0351
ENSG00000163629	PTPN13	-1.83	0.0314
ENSG00000169871	TRIM56	-1.83	0.00127
ENSG00000243789	JMJD7	-1.84	0.00188
ENSG00000267128	RNF157-AS1	-1.84	0.00105
ENSG00000128591	FLNC	-1.85	0.00135

ENSG00000228672	PROB1	-1.85	2.61E-6
ENSG00000225331	LOC101928576	-1.86	0.0374
ENSG00000226332	ADRM1	-1.87	4.99E-4
ENSG00000232063	LOC100132077	-1.87	4.39E-4
ENSG00000259974	LINC00261	-1.87	2.69E-4
ENSG00000258366	RTEL1	-1.88	0.00318
ENSG00000139908	TSSK4	-1.88	0.00219
ENSG00000182646	FAM156A/FAM156B	-1.88	3.93E-6
ENSG00000186174	BCL9L	-1.88	2.05E-6
ENSG00000204659	CBY3	-1.91	0.0131
ENSG00000127528	KLF2	-1.91	7.7E-10
ENSG00000179240	LOC100506127	-1.92	5.21E-9
ENSG00000075673	ATP12A	-1.93	0.0481
ENSG00000105227	PRX	-1.94	2.25E-4
ENSG00000177076	ACER2	-1.95	1.41E-5
ENSG00000122861	PLAU	-1.95	4.94E-8
ENSG00000234722	LINC01287	-1.96	0.0478
ENSG00000132405	TBC1D14	-1.96	0.00168
ENSG00000180776	ZDHHC20	-1.96	0.00114
ENSG00000229422	LOC100132249	-1.97	1.04E-4
ENSG00000259408	LOC101929988	-1.98	0.0363
ENSG00000254995	STX16-NPEPL1	-1.98	1.02E-4
ENSG00000185477	GPRIN3	-2.00	1.65E-9
ENSG00000172661	FAM21A/FAM21C	-2.01	8.69E-5
ENSG00000196622	RIMBP3 (includes others)	-2.01	5.95E-5
ENSG00000146247	PHIP	-2.02	5.14E-4
ENSG00000130382	MLLT1	-2.04	2.27E-5
ENSG00000215105	TTC3P1	-2.05	0.0154
ENSG00000215630	GUSBP9	-2.05	2.86E-5
ENSG00000096093	EFHC1	-2.06	0.00495
ENSG00000121281	ADCY7	-2.07	1.13E-9
ENSG00000258334	LOC101927267	-2.10	0.0191
ENSG00000213906	LTB4R2	-2.10	1.06E-8
ENSG00000185736	ADARB2	-2.11	0.0247
ENSG00000106006	HOXA6	-2.12	2.55E-5
ENSG00000212232	SNORD17	-2.13	0.00662
ENSG00000257315	ZBED6	-2.18	0.00222
ENSG00000170500	LONRF2	-2.19	0.00543
ENSG00000147145	LPAR4	-2.21	0.0278
ENSG00000107282	APBA1	-2.21	6.36E-5
ENSG00000235750	KIAA0040	-2.23	0.00184
ENSG00000251442	LINC01094	-2.24	0.00567
ENSG00000076382	SPAG5	-2.24	8.0E-6
ENSG00000102837	OLFM4	-2.25	0.00265
ENSG00000240303	ACAD11	-2.26	0.0043
ENSG00000157110	RBPMS	-2.27	9.3E-4
ENSG00000229780	UBE2Q1-AS1	-2.29	0.0257
ENSG00000140848	CPNE2	-2.32	0.032
ENSG00000264219	MIR4442	-2.35	0.00212
ENSG00000151276	MAGI1	-2.38	0.05
ENSG00000173482	PTPRM	-2.43	0.00161
ENSG00000246526	LOC339988	-2.43	2.55E-5
ENSG00000180229	HERC2P3	-2.45	0.00137
ENSG00000127588	GNG13	-2.46	7.52E-5
ENSG00000257594	GALNT4	-2.46	1.51E-8
ENSG00000179104	TMTC2	-2.49	0.0153
ENSG00000111796	KLRB1	-2.53	0.0345
ENSG00000111664	GNB3	-2.53	3.88E-6
ENSG00000145390	USP53	-2.56	0.00739
ENSG00000176994	SMCR8	-2.58	8.49E-6
ENSG00000215447	LOC642852	-2.60	0.00174
ENSG00000196535	MYO18A	-2.61	4.22E-5
ENSG00000231983	LINC00415	-2.62	0.00474
ENSG00000188822	CNR2	-2.63	0.0114
ENSG00000053438	NNAT	-2.66	0.0265
ENSG00000234857	HNRNPUL2-BSCL2	-2.70	1.19E-6
ENSG00000233539	LOC730338	-2.74	0.0045
ENSG00000185198	PRSS57	-2.84	0.0156
ENSG00000038382	TRIO	-2.84	0.0154
ENSG00000164292	RHOBTB3	-3.00	0.0492
ENSG00000180878	C11orf42	-3.08	0.0499

ENSG00000158683	PKD1L1	-3.08	0.0477
ENSG00000207704	mir-548	-3.08	0.043
ENSG00000107719	PALD1	-3.08	9.13E-5
ENSG00000187164	KIAA1598	-3.15	1.75E-4
ENSG00000005102	MEOX1	-3.16	0.0334
ENSG00000257489	GOLGA2P5	-3.17	0.00157
ENSG00000149634	SPATA25	-3.21	0.0296
ENSG00000171295	ZNF440	-3.27	0.0206
ENSG00000001630	CYP51A1	-3.31	0.00644
ENSG00000227268	KLLN	-3.39	0.0112
ENSG00000117114	LPHN2	-3.39	0.00982
ENSG00000184507	NUTM1	-3.43	0.0115
ENSG00000209418	SNORD64	-3.43	0.00951
ENSG00000145908	ZNF300	-3.45	0.0111
ENSG00000236529	DKFZP434F142	-3.56	0.00623
ENSG00000132563	REEP2	-3.79	0.0461
ENSG00000266235	MIR3176	-3.81	4.92E-5
ENSG00000074211	PPP2R2C	-3.89	5.42E-4
ENSG00000064835	POU1F1	-4.05	0.0193
ENSG00000177675	CD163L1	-4.28	0.0306
ENSG00000155016	CYP2U1	-4.5	0.0199
ENSG00000082397	EPB41L3	-4.52	1.55E-4
ENSG00000180071	ANKRD18A	-4.69	0.00625
ENSG00000151208	DLG5	-4.78	0.0244
ENSG00000179604	CDC42EP4	-5.13	0.0379
ENSG00000232850	PTGES2-AS1	-5.13	0.0327
ENSG00000077420	APBB1IP	-5.15	0.00745
ENSG00000149021	SCGB1A1	-5.24	0.0358
ENSG00000242808	SOX2-OT	-5.36	0.0283
ENSG00000260750	LOC101928737	-5.43	0.017
ENSG00000105501	SIGLEC5	-5.48	0.032
ENSG00000233968	LOC101928834	-5.56	0.0329
ENSG00000122707	RECK	-5.6	0.0384
ENSG00000239552	HOXB-AS2	-5.88	0.00105
ENSG00000128815	WDFY4	-5.94	0.00963
ENSG00000206952	SNORA76A	-6.00	3.32E-4
ENSG00000125810	CD93	-6.11	0.00604
ENSG00000151729	SLC25A4	-6.34	0.0311
ENSG00000221866	PLXNA4	-6.92	0.0317
ENSG00000246363	LOC728084	-7.11	0.0106
ENSG00000105492	SIGLEC6	-7.14	0.0279
ENSG00000198417	MT1F	-7.45	0.0244
ENSG00000116191	RALGPS2	-7.66	0.0215
ENSG00000173372	C1QA	-7.77	0.0206
ENSG00000176273	SLC35G1	-7.90	0.019
ENSG00000172179	PRL	-7.93	0.019
ENSG00000175893	ZDHHC21	-8.03	0.0177
ENSG00000137573	SULF1	-8.32	0.00373
ENSG00000170085	SIMC1	-8.75	0.00945
ENSG00000120008	WDR11	-8.91	5.91E-4
ENSG00000146950	SHROOM2	-10.7	0.00687
ENSG00000221957	KIR2DS4 (includes others)	-11.3	0.00629
ENSG00000125498	KIR2DL1/KIR2DL3	-12.4	0.00784

Common genes for KIR2DS1_4h and NKG2D_4h stimulation:

Ensembl ID	Gene symbol	Fold change (KIR2DS1_4h)	p-value (KIR2DS1_4h)	Fold change (NKG2D_4h)	p-value (NKG2D_4h)
ENSG00000179388	EGR3 (transcription factor)	3.94	2.66E-20	3.01	0.0000000675
ENSG00000114423	CBLB (E3 ubiquitin ligase)	2.14	5.06E-36	1.93	1.15E-43
ENSG00000140199	SLC12A6 (K-Cl transporter)	1.90	4.2E-14	2.13	3.15E-31
ENSG00000102908	NFAT5	1.88	2.64E-86	1.66	1.35E-59
ENSG00000109320	NFKB1	1.81	4.12E-71	1.51	5.33E-67
ENSG00000153094	BCL2L11	1.76	6.5E-6	1.53	6.46E-7
ENSG00000135048	TMEM2	1.72	1.95E-29	1.51	8.15E-36
ENSG00000235724	LOC101929512	1.68	0.00232	1.58	0.000485
ENSG00000226312	CFLAR-AS1	1.56	0.0249	1.53	0.00648

Common genes for KIR2DS1_4h and Ly49H_4h stimulation:

Ensembl ID	Gene symbol	Fold change (KIR2DS1_4h)	p-value (KIR2DS1_4h)	Fold change (Ly49H_4h)	p-value (Ly49H_4h)
ENSG00000204671	IL31	5.13	0.00468	7.65	2.02E-19

ENSG00000164399	IL3	3.92	8.91E-6	6.76	1.27E-29
ENSG00000006074	CCL18	3.62	0.00479	3.73	0.000837
ENSG00000233791	LINC01136	2.39	0.0191	3.30	1.54E-5
ENSG00000249241	LOC101060498	2.28	0.0129	2.42	0.00274
ENSG00000171552	BCL2L1	2.10	7.79E-94	1.56	2.41E-26
ENSG00000222009	BTBD19	2.03	3.13E-4	2.78	2.11E-11
ENSG00000067208	EVI5	1.84	4.78E-30	2.51	1.31E-46
ENSG00000109787	KLF3	1.83	1.44E-4	2.13	2.49E-5
ENSG00000253522	mir-146	1.83	5.6E-11	1.57	1.09E-6
ENSG00000215417	MIR17HG	1.83	6.21E-21	1.86	5.45E-19
ENSG00000104783	KCNN4	1.80	8.4E-48	1.75	8.91E-21
ENSG00000146232	NFKBIE	1.80	3.65E-66	2.46	2.56E-61
ENSG00000101849	TBL1X	1.80	7.18E-4	-5.33	0.0353
ENSG00000182687	GALR2	1.77	0.0262	2.17	0.00428
ENSG00000155974	GRIP1	1.77	0.0204	2.83	3.12E-7
ENSG00000144802	NFKBIZ	1.77	4.37E-20	1.91	2.19E-19
ENSG00000213443	CLEC2D	1.71	1.88E-39	2.01	4.3E-22
ENSG00000186594	MIR22HG	1.71	1.14E-17	2.84	8.85E-49
ENSG00000069399	BCL3	1.68	1.17E-50	2.25	3.48E-45
ENSG00000162783	IER5	1.67	5.59E-19	1.72	2.46E-10
ENSG00000179294	C17orf96	1.66	6.36E-34	1.81	1.01E-21
ENSG00000145779	TNFAIP8	1.66	1.26E-60	1.90	1.3E-33
ENSG00000099860	GADD45B	1.65	2.12E-35	1.59	8.93E-22
ENSG00000008405	CRY1	1.62	9.82E-50	1.78	1.66E-34
ENSG00000120278	PLEKHG1	1.62	0.0342	1.95	0.00539
ENSG00000264577	SNORD4A	1.60	0.00608	1.95	1.02E-4
ENSG00000256594	LOC374443	1.58	7.3E-25	1.89	1.16E-26
ENSG00000165997	ARL5B	1.57	8.75E-48	2.09	8.7E-55
ENSG00000174749	C4orf32	1.57	1.17E-44	1.81	3.4E-31
ENSG00000138166	DUSP5	1.56	1.35E-13	1.83	2.29E-14
ENSG00000006327	TNFRSF12A	1.56	3.85E-14	1.69	3.68E-14
ENSG00000117560	FASLG	1.55	8.29E-21	2.10	4.14E-30
ENSG00000095794	CREM	1.52	2.23E-27	2.00	5.31E-22
ENSG00000215244	LOC399715	1.52	0.0332	2.09	6.52E-5
ENSG00000087074	PPP1R15A	1.52	6.43E-11	1.61	7.04E-10
ENSG00000118515	SGK1	1.52	4.46E-13	2.85	6.92E-44
ENSG00000125733	TRIP10	1.51	3.26E-46	1.71	4.26E-29
ENSG00000121807	CCR2	-1.56	3.28E-35	-2.12	4.83E-26
ENSG00000241978	AKAP2	-1.57	0.00476	-3.41	2.28E-8
ENSG00000140836	ZFHX3	-1.57	0.0105	-1.74	0.00618
ENSG00000172349	IL16	-1.62	2.88E-5	-1.52	5.03E-4
ENSG00000213626	LBH	-1.62	9.31E-11	-1.60	4.47E-6
ENSG00000164855	TMEM184A	-1.62	5.11E-4	-2.19	0.0123
ENSG00000261064	LOC100996255	-1.67	0.033	-4.06	1.22E-5
ENSG00000262312	LOC101929732	-1.82	3.14E-4	-4.53	1.58E-11
ENSG00000211696	TRGV8	-1.82	7.78E-5	-1.53	0.00124
ENSG00000235172	LINC01366	-1.83	1.69E-7	-1.67	5.34E-5
ENSG00000188626	GOLGA8J (includes others)	-1.86	3.69E-4	-5.43	0.0116
ENSG00000091831	ESR1	-2.14	0.00287	-3.14	5.88E-5
ENSG00000226650	KIF4B	-2.27	5.66E-5	-2.35	1.38E-4

Common genes for Ly49H_4h and NKG2D_4h stimulation:

Ensembl ID	Gene symbol	Fold change (Ly49H_4h)	p-value (Ly49H_4h)	Fold change (NKG2D_4h)	p-value (NKG2D_4h)
ENSG00000112115	IL17A	6.49	4.39E-10	5.47	9.0E-6
ENSG00000122641	INHBA	6.34	3.96E-67	1.88	0.0172
ENSG00000117009	KMO	5.93	1.38E-16	3.12	0.00839
ENSG00000146216	TTBK1	4.94	0.00442	5.57	6.14E-5
ENSG00000130202	PVRL2	4.17	2.75E-34	2.50	1.12E-6
ENSG00000177494	ZBED2	3.03	6.92E-26	1.95	4.84E-9
ENSG00000236700	LINC01010	2.92	0.00985	2.43	0.042
ENSG00000173077	Dec-1	2.65	1.41E-26	1.57	1.12E-5
ENSG00000167772	ANGPTL4	2.43	0.00289	1.90	0.0341
ENSG00000197208	SLC22A4	2.31	0.00449	1.86	0.0145
ENSG00000231346	LINC01160	2.25	7.22E-17	1.91	3.08E-18
ENSG00000240240	LOC101060026	2.22	1.55E-4	1.60	0.0058

Common genes for KIR2DS1_4h, Ly49H_4h, and NKG2D_4h stimulation:

Ensembl ID	Gene symbol	Fold change (KIR2DS1_4h)	p-value (KIR2DS1_4h)	Fold change (Ly49H_4h)	p-value (Ly49H_4h)	Fold change (NKG2D_4h)	p-value (NKG2D_4h)
ENSG00000168334	XIRP1	9.99	7.94E-66	12.30	1.61E-152	9.66	8.94E-95

ENSG00000138684	IL21	8.40	1.53E-24	7.25	6.47E-17	6.60	1.62E-11
ENSG00000109943	CRTAM	8.16	2.17E-151	10.40	1.79E-252	8.13	2.09E-136
ENSG00000129277	CCL4	8.04	7.84E-199	10.00	1.25E-145	7.74	1.18E-228
ENSG00000169429	CXCL8	7.98	1.16E-263	10.50	3.07E-259	6.78	8.15E-281
ENSG00000108702	CCL1	7.90	3.16E-42	7.52	3.87E-89	6.80	1.27E-23
ENSG00000197262	CCL4L1/CCL4L2	7.65	4.13E-23	10.10	4.69E-84	6.78	3.67E-15
ENSG00000164400	CSF2	7.53	5.41E-148	10.30	5.73E-243	5.86	5.58E-32
ENSG00000006075	CCL3	7.50	5.11E-239	9.63	5.18E-198	7.07	4.18E-252
ENSG00000205021	CCL3L1	7.41	2.02E-42	10.60	2.52E-91	5.19	2.57E-12
ENSG00000128342	LIF	7.24	1.65E-235	9.06	1.83E-293	6.63	7.41E-210
ENSG00000109471	IL2	7.03	1.79E-49	11.50	1.02E-86	5.22	2.75E-19
ENSG00000111537	IFNG	6.48	0.00	8.89	8E-305	5.81	0.00
ENSG00000232810	TNF	6.44	8.57E-74	8.97	3.92E-162	5.57	3.08E-44
ENSG00000135625	EGR4	6.28	7.5E-284	6.07	5.25E-169	5.49	7.41E-210
ENSG00000124145	SDC4	5.69	1.28E-51	6.35	1.68E-75	5.05	2.39E-37
ENSG00000050730	TNIP3	5.58	4.31E-220	5.47	3.24E-133	5.44	3.84E-193
ENSG00000125740	FOSB	5.53	4.63E-262	5.52	1.02E-101	4.86	5.58E-258
ENSG00000143184	XCL1	5.52	9.47E-248	7.78	5.34E-203	5.39	2.02E-195
ENSG00000170345	FOS	5.45	5.05E-177	5.51	8.39E-126	4.68	9.51E-77
ENSG00000115598	IL1RL2	5.32	6.65E-4	4.95	0.0047	4.88	6.82E-4
ENSG00000227145	IL21-AS1	5.32	6.83E-4	6.55	1.41E-10	5.81	2.82E-8
ENSG00000108691	CCL2	5.16	1.44E-84	5.32	3.64E-106	4.06	1.05E-29
ENSG00000119508	NR4A3	4.93	1.03E-70	5.48	8.42E-79	4.56	3.79E-80
ENSG00000120738	EGR1	4.88	1.07E-195	4.99	4.05E-122	4.20	8.98E-88
ENSG00000122877	EGR2	4.81	5.34E-99	5.10	1.4E-90	4.41	2.68E-101
ENSG00000145839	IL9	4.51	1.3E-8	6.66	4.01E-28	3.08	0.00112
ENSG00000143185	XCL2	4.42	2.57E-8	3.97	3.58E-6	3.43	4.99E-5
ENSG00000049249	TNFRSF9	4.33	1.7E-57	3.69	5.01E-33	4.10	4.32E-53
ENSG00000167874	TMEM88	4.19	2.18E-17	6.78	6.81E-49	3.64	3.88E-17
ENSG00000106366	SERPINE1	4.14	8.77E-15	4.78	3.33E-23	2.98	2.97E-7
ENSG00000123358	NR4A1	4.06	7.35E-158	4.25	2.05E-104	3.63	6.25E-131
ENSG00000134668	SPOCD1	4.01	1.86E-6	4.39	1.49E-8	3.45	1.37E-5
ENSG00000236453	LOC102723946	3.96	2.9E-13	4.66	6.67E-23	3.13	7.2E-10
ENSG00000109321	AREG	3.95	1.32E-33	5.50	8.33E-83	3.79	6.1E-37
ENSG00000162692	VCAM1	3.95	5.4E-37	2.43	4.53E-8	2.78	2.68E-19
ENSG00000143333	RGS16	3.86	3.1E-6	3.41	1.11E-5	3.44	8.06E-7
ENSG00000132510	KDM6B	3.78	8.28E-171	3.87	4.81E-107	3.50	8.18E-162
ENSG00000118503	TNFAIP3	3.77	4.8E-56	4.06	1.24E-54	3.51	2.26E-53
ENSG00000256515	CCL3L3	3.75	0.0409	8.03	1.25E-31	3.46	0.0162
ENSG00000140379	BCL2A1	3.73	1.18E-139	4.95	8E-103	3.29	5.75E-107
ENSG00000185022	MAFF	3.69	2.31E-86	4.64	5.21E-99	3.19	7.58E-92
ENSG00000136367	ZFHX2	3.62	8.15E-45	3.17	1.85E-25	3.36	1.29E-45
ENSG00000125730	C3	3.58	2.79E-15	3.68	1.64E-14	2.96	6.95E-13
ENSG00000144655	CSRNP1	3.57	1.23E-186	4.62	8.26E-104	3.10	7E-201
ENSG00000184545	DUSP8	3.57	4.81E-13	3.95	4.99E-17	3.43	1.06E-16
ENSG00000166592	RRAD	3.48	1.46E-11	4.71	1.73E-21	2.39	7.98E-5
ENSG00000056558	TRAF1	3.4	9.46E-152	3.79	5.73E-119	3.02	5.64E-110
ENSG00000100906	NFKBIA	3.38	6.38E-61	4.09	1.5E-75	2.64	2.73E-52
ENSG00000197461	PDGFA	3.38	9.49E-45	3.32	1.36E-35	2.76	1.98E-43
ENSG00000167604	NFKBID	3.35	6.64E-225	4.31	4.48E-82	2.68	1.07E-215
ENSG00000230533	LOC102723649	3.31	2.27E-6	4.96	7.22E-17	2.74	3.33E-4
ENSG00000153234	NR4A2	3.29	8.7E-76	4.01	4.78E-93	3.05	4.33E-46
ENSG00000234883	MIR155HG	3.27	3.23E-27	4.25	1.12E-43	2.48	2.82E-20
ENSG00000199568	RNU5A-1	3.27	5.2E-16	4.10	2.76E-29	2.57	5.59E-6
ENSG00000090339	ICAM1	3.23	2.27E-107	3.38	2.03E-65	2.46	7.89E-74
ENSG00000166920	C15orf48	3.18	0.00549	4.12	4.68E-7	2.76	0.0182
ENSG00000121101	TEX14	3.12	2.91E-27	3.91	3.04E-42	2.48	6.47E-20
ENSG00000187556	NANOS3	3.09	0.00217	3.04	0.00442	2.43	0.0353
ENSG00000023445	BIRC3	3.05	2.2E-56	2.88	2.36E-38	2.70	3.64E-63
ENSG00000125657	TNFSF9	3.05	3.94E-6	6.03	4.89E-58	3.26	1.78E-10
ENSG00000120217	CD274	2.99	8.16E-47	3.38	2.19E-38	2.70	1.35E-52
ENSG00000108924	HLF	2.97	6.52E-22	3.78	1.48E-35	2.44	5.66E-20
ENSG00000105835	NAMPT	2.92	1.68E-198	3.28	1.61E-130	2.56	4.86E-176
ENSG00000131669	NINJ1	2.87	2.16E-88	3.56	4.3E-59	2.29	2.7E-68
ENSG00000159388	BTG2	2.84	1.17E-61	3.80	8.46E-70	2.40	3.11E-63
ENSG00000105246	EBI3	2.79	2.31E-9	2.63	8.46E-10	1.93	5.91E-7
ENSG00000170542	SERPINB9	2.78	1.38E-110	3.20	3.64E-106	2.58	2.11E-98
ENSG00000172738	TMEM217	2.77	1.49E-47	3.40	5.77E-47	2.36	2.74E-39
ENSG00000166886	NAB2	2.72	2.18E-148	1.54	8.12E-10	2.48	6.83E-126
ENSG00000100453	GZMB	2.68	5.33E-45	4.65	1.84E-65	2.85	1.35E-60
ENSG00000134030	CTIF	2.67	6.34E-5	2.87	7.89E-6	2.26	4.56E-5

ENSG00000177606	JUN	2.67	4.03E-33	2.13	1.45E-15	1.91	1.54E-23
ENSG00000240057	LOC102724287	2.61	5.8E-6	1.99	0.0146	1.82	0.00518
ENSG00000164287	CDC20B	2.59	8.32E-9	3.25	3.7E-16	1.81	1.18E-4
ENSG00000114473	IQCG	2.58	3.73E-90	3.02	2.03E-67	2.13	4.52E-87
ENSG00000173334	TRIB1	2.58	6.66E-21	2.86	3.11E-24	2.18	1.98E-20
ENSG00000104951	IL4I1	2.57	5.02E-14	3.32	2.75E-23	2.34	1.04E-11
ENSG00000168389	MFSD2A	2.56	1.61E-148	2.69	3.04E-75	2.12	4.46E-97
ENSG00000104856	RELB	2.47	2.88E-20	2.86	8.33E-24	2.11	9.54E-22
ENSG00000162772	ATF3	2.45	1.09E-63	3.14	4.39E-91	1.91	9.91E-71
ENSG00000184557	SOCS3	2.45	1.29E-44	3.22	6.23E-68	1.89	1.16E-32
ENSG00000180209	MYLPF	2.44	9.64E-4	2.74	7.78E-4	1.75	0.0356
ENSG00000110848	CD69	2.43	8.04E-40	3.14	6.18E-54	2.00	1.18E-44
ENSG00000174946	GPR171	2.43	9.87E-29	2.34	1.71E-24	2.05	3.68E-24
ENSG00000149289	ZC3H12C	2.43	2.89E-106	2.99	8.42E-79	2.26	5.24E-102
ENSG00000137331	IER3	2.39	1.68E-62	3.60	2.7E-59	1.75	1.31E-40
ENSG00000207870	mir-221	2.39	1.54E-8	2.99	2.68E-16	1.78	1.22E-6
ENSG00000162924	REL	2.38	4.57E-44	1.54	3.85E-6	2.63	4.14E-46
ENSG00000171604	CXXC5	2.36	1.08E-12	2.18	2.9E-14	1.87	5.72E-12
ENSG00000171223	JUNB	2.33	2.2E-113	2.76	3.92E-87	1.86	4.21E-98
ENSG00000112149	CD83	2.30	5.44E-54	2.89	4.99E-62	1.99	1.53E-56
ENSG00000160606	TLCD1	2.29	5.71E-44	2.94	7.12E-23	1.76	1.16E-32
ENSG00000267534	S1PR2	2.27	1.24E-43	2.86	8.17E-36	1.83	6.79E-19
ENSG00000007866	TEAD3	2.27	2.84E-9	2.62	2.7E-12	2.41	3.28E-10
ENSG00000197019	SERTAD1	2.26	7.08E-70	3.18	5.72E-38	1.82	1.24E-57
ENSG00000155090	KLF10	2.23	2.31E-60	1.68	1.2E-16	1.71	7.92E-58
ENSG00000221887	HMSD	2.19	8.3E-14	2.88	3.64E-26	1.91	1.69E-10
ENSG00000198355	PIM3	2.16	1.85E-98	2.49	8.99E-76	1.72	2.1E-90
ENSG00000124762	CDKN1A	2.14	2.05E-24	3.64	9.13E-75	1.91	6.49E-19
ENSG00000011590	ZBTB32	2.14	4.02E-83	2.28	7.23E-29	1.78	2.79E-48
ENSG00000226380	mir-29	2.11	6.17E-23	3.57	2.07E-46	1.94	3.94E-29
ENSG00000169398	PTK2	2.09	9.5E-6	2.16	7.26E-5	1.62	7.68E-5
ENSG00000123146	CD97	2.06	1.38E-109	1.85	6.38E-34	1.61	1.54E-71
ENSG00000119772	DNMT3A	2.06	6.1E-13	1.86	6.83E-8	1.70	8.91E-10
ENSG00000161570	CCL5	2.05	1.98E-41	3.06	3.3E-53	1.83	1.42E-36
ENSG00000088899	LZTS3	2.03	5.87E-36	1.63	1.64E-14	1.57	2.23E-19
ENSG00000095637	SORBS1	2.03	5.07E-14	2.17	3.09E-9	2.00	4.35E-12
ENSG00000185650	ZFP36L1	2.03	9.79E-63	2.87	9.85E-53	1.73	2.83E-35
ENSG00000023902	PLEKHO1	2.02	2.42E-5	1.95	0.00185	1.56	2.95E-4
ENSG00000175183	CSRP2	1.99	0.0313	2.03	0.0231	1.74	0.0212
ENSG00000136052	SLC41A2	1.99	4.88E-33	2.14	1.64E-29	1.60	1.54E-28
ENSG00000117586	TNFSF4	1.99	2.15E-86	1.88	1.04E-40	1.61	7.83E-71
ENSG00000077150	NFKB2	1.98	1.63E-19	2.38	9.86E-21	1.82	2.76E-24
ENSG00000137502	RAB30	1.97	2.64E-50	1.73	5.69E-21	1.69	1.34E-36
ENSG00000136244	IL6	1.93	0.00177	4.30	4.24E-37	1.66	0.000627
ENSG00000125735	TNFSF14	1.92	1.52E-62	2.27	2.99E-28	1.51	1.06E-38
ENSG00000003402	CFLAR	1.90	1.5E-86	2.06	9.03E-40	1.75	9.6E-79
ENSG00000231507	LINC01353	1.90	8.01E-8	3.07	1.49E-24	1.86	7.01E-11
ENSG00000173166	RAPH1	1.90	1.56E-7	2.61	1.79E-11	1.77	2.96E-8
ENSG00000163874	ZC3H12A	1.89	1.78E-39	2.07	2.52E-36	1.52	8.15E-43
ENSG00000126561	STAT5A	1.88	2.52E-69	1.82	1.82E-29	1.55	1.06E-34
ENSG00000075426	FOSL2	1.87	5.96E-28	2.09	2.2E-25	1.78	3.07E-39
ENSG00000150977	RILPL2	1.87	3.24E-70	1.55	6.75E-23	1.57	1.59E-63
ENSG00000253210	LOC101927963	1.81	3.79E-21	3.5	1.5E-54	2.05	2.34E-33
ENSG00000076604	TRAF4	1.81	1.92E-52	1.99	1.06E-41	1.52	5.4E-46
ENSG00000143669	LYST	1.79	1.16E-39	1.63	4.11E-20	1.82	3.13E-44
ENSG00000130449	ZSWIM6	1.79	3.22E-56	1.66	6.15E-20	1.66	1.39E-77
ENSG00000197329	PELI1	1.73	1.22E-78	1.89	2.09E-36	1.53	7.36E-83
ENSG00000171174	RBKS	1.68	1.52E-4	2.64	4.98E-16	1.89	1.02E-14
ENSG00000140564	FURIN	1.66	1.79E-7	1.66	1.02E-6	1.60	4.36E-8
ENSG00000166455	C16orf46	1.50	8.56E-5	1.77	2.18E-6	1.83	6.37E-13
ENSG00000090104	RGS1	1.50	3.69E-35	2.50	4.57E-41	1.53	5.3E-33